UNIVERSIDADE ESTADUAL PAULISTA JÚLIO DE MESQUITA FILHO
FACULDADE DE CIÊNCIAS AGRÁRIAS E VETERINÁRIAS
CAMPUS DE JABOTICABAL

EFEITO DA EXPOSIÇÃO AO ÁCARO DA POEIRA DOMÉSTICA NA QUIMIOSSENSIBILIDADE CENTRAL E PERIFÉRICA EM MODELO MURINO DE ASMA

Beatriz Dominiquini Moraes

Médica Veterinária

2026

UNIVERSIDADE ESTADUAL PAULISTA JÚLIO DE MESQUITA FILHO
FACULDADE DE CIÊNCIAS AGRÁRIAS E VETERINÁRIAS
CAMPUS DE JABOTICABAL

EFEITO DA EXPOSIÇÃO AO ÁCARO DA POEIRA DOMÉSTICA NA QUIMIOSSENSIBILIDADE CENTRAL E PERIFÉRICA EM MODELO MURINO DE ASMA

Beatriz Dominiquini Moraes

Orientadora: Profa. Dra. Luciane Helena Gargaglioni Batalhão

Dissertação apresentada à Faculdade de Ciências Agrárias e Veterinárias FCAV–UNESP, Câmpus de Jaboticabal, como parte das exigências para obtenção do título de Mestre em Ciência Animal com Ênfase em Fisiologia e Bem-Estar Animal.

2026

D671e

Dominiquini-Moraes, Beatriz
Efeito da exposição ao ácaro da poeira doméstica na quimiossensibilidade central e periférica em modelo murino de asma / Beatriz Dominiquini-Moraes. -- Jaboticabal, 2026
73 p. : il., tabs., fotos

Dissertação (mestrado) - Universidade Estadual Paulista (UNESP), Faculdade de Ciências Agrárias e Veterinárias, Jaboticabal
Orientadora: Luciane Helena Gargaglioni

1. Fisiologia. 2. Fisiologia experimental. 3. Fisiopatologia. 4. Metabolismo. I. Título.

Sistema de geração automática de fichas catalográficas da Unesp. Dados fornecidos pelo autor(a).

UNIVERSIDADE ESTADUAL PAULISTA

Câmpus de Jaboticabal

CERTIFICADO DE APROVAÇÃO

TÍTULO DA DISSERTAÇÃO: EFEITO DA EXPOSIÇÃO AO ÁCARO DA POEIRA DOMÉSTICA NA QUIMIOSSENSIBILIDADE EM MODELO MURINO DE ASMA

AUTORA: BEATRIZ DOMINIQUINI MORAES
ORIENTADORA: LUCIANE HELENA GARGAGLIONI BATALHÃO

Aprovada como parte das exigências para obtenção do Título de Mestra em Ciência Animal, área: Fisiologia e Bem Estar Animal pela Comissão Examinadora:

gov.br Documento assinado digitalmente
LUCIANE HELENA GARGAGLIONI BATALHAO
Data: 28/05/2026 18:07:47-0300
Verifique em https://validar.iti.gov.br

Profa. Dra. LUCIANE HELENA GARGAGLIONI BATALHÃO (Participaçao Presencial)
Departamento de Morfologia e Fisiologia Animal / UNESP / Câmpus de Jaboticabal - FCAV

gov.br Documento assinado digitalmente
CAROLINE MARCANTONIO FERREIRA
Data: 28/05/2026 18:57:38-0300
Verifique em https://validar.iti.gov.br

Profa. Dra. CAROLINE MARCANTONIO FERREIRA (Participaçao Virtual)

gov.br Documento assinado digitalmente
LUANA TENORIO LOPES
Data: 28/05/2026 18:27:12-0300
Verifique em https://validar.iti.gov.br

Pesquisadora Dra. LUANA TENÓRIO LOPES (Participaçao Virtual)
Departamento de Morfologia e Fisiologia Animal / FCAV / UNESP - Jaboticabal

Jaboticabal, 28 de maio de 2026.

DADOS CURRICULARES DO AUTOR

Beatriz Dominiquini Moraes, nascida em 20 de abril de 2000 na cidade de Alfenas – MG, filha de José Pedro Ferreira Moraes e Zenaide Dominiquini Moraes. Graduada em Medicina Veterinária pela Universidade Estadual Paulista (UNESP), Faculdade de Ciências Agrárias e Veterinárias de Jaboticabal (FCAV). Foi bolsista da FAPESP durante a iniciação científica, em pesquisa sobre o efeito do ciclo estral e o papel da progesterona na resposta ventilatória hipercápnica e na expressão de comportamentos relacionados ao pânico, no laboratório de Fisiologia Respiratória do Departamento de Morfologia e Fisiologia Animal da UNESP-FCAV, sob orientação da Profa. Dra. Luciane Helena Gargaglioni Batalhão. É bolsista do CNPq e realiza mestrado acadêmico no Programa de Pós-Graduação em Ciência Animal da UNESP-FCAV, sob orientação da Profa. Dra. Luciane Helena Gargaglioni Batalhão.

Por vezes sentimos que aquilo que fazemos não é senão uma gota de água no mar. Mas o mar seria menor se lhe faltasse uma gota.

– Madre Teresa de Calcutá

Dedico este trabalho à minha mãe e minha avó, exemplos de força e resiliência, que me inspiram diariamente a seguir em frente diante dos desafios.

AGRADECIMENTOS

Agradeço, primeiramente, aos meus pais e a toda a minha família, por todo o amor, incentivo e suporte incondicional ao longo desta jornada. Há oito anos, deixei minha cidade para vir a Jaboticabal em busca do sonho de cursar o ensino superior, e em nenhum momento me faltaram apoio, confiança ou palavras de encorajamento. Mesmo à distância, vocês estiveram presentes em cada conquista e em cada desafio, tornando este caminho mais leve e possível. Agradeço por acreditarem em mim mesmo nos momentos em que eu duvidei das minhas próprias capacidades, por compreenderem as ausências, as preocupações e as dificuldades inerentes à vida acadêmica, e por celebrarem comigo cada pequena vitória ao longo desses anos. Tudo o que conquistei até aqui carrega um pouco do esforço, da dedicação e do amor de vocês. À minha mãe e à minha avó, em especial, deixo minha profunda gratidão por serem exemplos de força, resiliência e determinação. Seus ensinamentos e suas trajetórias de vida sempre foram fonte de inspiração e motivação para que eu seguisse em frente diante dos desafios. Esta conquista também é de vocês. Muito obrigada por tornarem possível a realização deste sonho.

Agradeço também aos amigos que encontrei ao longo desta jornada, aos que permaneceram ao meu lado após o término da graduação e aos novos que o mestrado me proporcionou. A vocês, deixo minha sincera gratidão. Obrigada por cada conversa, cada risada, cada gesto de amizade e por toda ajuda oferecida sempre que precisei. Em especial, agradeço à Natália por cada lâmina cortada após o horário de expediente até mesmo na ausência de luz; por toda a paciência nos momentos em que foi necessário repetir o protocolo; e pela disposição constante em ajudar independente de sua rotina com a residência. Você foi fundamental para a realização deste trabalho, parte dele não teria sido possível sem você. À Sofia, agradeço por um gesto de generosidade que teve um significado imensurável no início da nossa trajetória na pós-graduação, quando ainda enfrentávamos as incertezas e dificuldades do período sem bolsa. Seu apoio representou muito mais do que uma ajuda pontual; foi um gesto de empatia, acolhimento e companheirismo que levarei para sempre comigo com enorme carinho e gratidão.

Agradeço a todos os alunos do laboratório, pelas vivências compartilhadas ao longo desses anos e pela disposição em ajudar sempre que necessário. Agradeço também à professora Alexandra Ivo de Medeiros e às suas alunas, em especial Luiza e Fernanda, pelo suporte com o protocolo de ELISA. A contribuição de vocês foi fundamental para a realização desta etapa do trabalho.

Por fim, mas não menos importante, agradeço à minha orientadora, Luciane Gargaglioni, por ter acreditado em mim desde o início da minha trajetória no laboratório, ainda em 2020, durante a graduação. Mesmo diante de uma rotina intensa de aula, você me deu a oportunidade de ingressar na pesquisa científica e confiou no meu potencial para desenvolver uma iniciação científica e, anos depois, um mestrado. Agradeço pela orientação, pelos ensinamentos, pela confiança depositada em mim e por todas as oportunidades de crescimento que me proporcionou ao longo desses anos. Sua dedicação à ciência e seu comprometimento com a formação de seus alunos são inspirações para todos nós que trabalhamos ao seu lado. Muito obrigada!

Agradeço à Coordenação de Aperfeiçoamento de Pessoal de Nível Superior e ao Conselho Nacional de Desenvolvimento Científico e Tecnológico pela concessão da bolsa de estudo e pelo apoio financeiro que possibilitou a realização deste trabalho.

SUMÁRIO

EFEITO DA EXPOSIÇÃO AO ÁCARO DA POEIRA DOMÉSTICA NA QUIMIOSSESIBILIDADE CENTRAL E PERIFÉRICA EM MODELO MURINO DE ASMA

RESUMO – A asma alérgica é uma condição inflamatória crônica das vias aéreas. Evidências crescentes sugerem que a inflamação associada à asma pode desestabilizar o sistema de controle respiratório, favorecendo a ocorrência de comorbidades e agravando o curso da doença. Nesse contexto, o presente estudo teve como objetivo investigar a quimiossensibilidade central e periférica em um modelo murino de inflamação alérgica das vias aéreas. Para isso, camundongos C57BL/6 machos e fêmeas foram expostos ao ácaro da poeira doméstica (HDM), e seus padrões ventilatório e metabólico foram avaliados em condições de ar ambiente, hipóxia (7% O_2) e hipercapnia (7% CO_2). A exposição ao HDM promoveu alterações sexo-específicas no padrão ventilatório em ar ambiente, com aumento da frequência respiratória (f_R) nos machos, enquanto nas fêmeas foi observada redução do metabolismo basal, evidenciada pela diminuição do consumo de O_2 (VO_2). Durante a hipóxia, os machos expostos ao HDM apresentaram resposta ventilatória aumentada, caracterizada por maior f_R, ventilação-minuto (V_E) e equivalente respiratório de O_2 (V_E/VO_2); enquanto as fêmeas apresentaram resposta reduzida, com aumento do VO_2 e diminuição do V_E/VO_2. Na hipercapnia, os machos expostos ao HDM apresentaram menor resposta ventilatória, associada ao aumento do VO_2 e à redução do V_E/VO_2, enquanto nas fêmeas observou-se aumento do VO_2, sem alteração do V_E/VO_2. Em conjunto, nossos dados sugerem que a inflamação alérgica induzida pelo HDM promove alterações sexo-dependentes no metabolismo basal e na resposta quimiossensorial periférica e central.

Palavras-chave: inflamação, quimiorreflexo, hipercapnia, hipóxia.

ALLERGIC AIRWAY INFLAMMATION INDUCES SEX-SPECIFIC ALTERATIONS IN CHEMOREFLEX FUNCTION AND METABOLISM IN MICE

ABSTRACT – Allergic asthma is a chronic inflammatory disease of the airways. Growing evidence suggests that asthma-associated inflammation may destabilize the respiratory control system, thereby promoting the occurrence of comorbidities and worsening disease progression. In this context, the present study aimed to investigate central and peripheral chemosensitivity in a murine model of allergic airway inflammation. For this purpose, male and female C57BL/6 mice were exposed to house dust mites (HDM), and their ventilatory and metabolic patterns were assessed under room air, hypoxia (7% O_2), and hypercapnia (7% CO_2). HDM exposure induced sex-specific alterations in ventilatory patterns under room-air conditions, with an increase in respiratory frequency (f_R) in males, whereas females exhibited a reduction in basal metabolic rate, as evidenced by decreased oxygen consumption (VO_2). During hypoxia, HDM-exposed males showed an enhanced ventilatory response, characterized by increased f_R, minute ventilation (V_E), and ventilatory equivalent for O_2 (V_E/VO_2), whereas females displayed a blunted response, with increased VO_2 and decreased V_E/VO_2. Under hypercapnic conditions, HDM-exposed males exhibited a reduced ventilatory response, with increased VO_2 and decreased V_E/VO_2, whereas females showed increased VO_2 without changes in V_E/VO_2. Taken together, our findings suggest that HDM-induced allergic inflammation promotes sex-dependent alterations in basal metabolism and differentially modulates peripheral and central chemosensory responses.

Keywords: asthma, chemosensitivity, hypercapnia, hypoxia.

CAPÍTULO 1 – CONSIDERAÇÕES GERAIS

1. INTRODUÇÃO

A asma é uma condição inflamatória crônica das vias aéreas, caracterizada por alterações estruturais que levam à obstrução e hiperresponsividade (GINA, 2020). Em 2019, foi estimado que cerca de 262 milhões de pessoas eram acometidas pela doença em todo o mundo, responsável por 461.000 mortes, segundo o estudo Global Burden of Disease (IHME, 2024). A prevalência varia em função da idade e do sexo, sendo mais comum em meninos na infância, enquanto as mulheres são mais afetadas na idade adulta, sugerindo que os hormônios sexuais desempenham um papel de destaque na manifestação da doença (Cephus et al., 2017; Dharmage et al., 2019; Stern et al., 2020).

Dada a heterogeneidade das manifestações clínicas, a asma pode ser classificada quanto ao fenótipo: alérgico ou não alérgico (Hammad e Lembrecht, 2021). A asma alérgica é o fenótipo mais comum e tende a começar na infância (Levy et al., 2023). A patogenia caracteriza-se pela ativação de linfócitos T auxiliares do tipo 2 em resposta à sensibilização por alérgenos ambientais, como ácaros, pólen e pelo de animais (Hammad e Lembrecht, 2021). Os sintomas decorrem da reação inflamatória mediada principalmente pelas interleucinas (IL) 4, IL-5 e IL-13, que desempenham um papel fundamental na reação alérgica inicial (Hammad e Lembrecht, 2021). O conjunto desses mecanismos culmina no remodelamento das vias aéreas, com acúmulo de muco e hipertrofia e hiperplasia da musculatura lisa, que causa quadros de broncoconstrição reversível (Agache et al., 2012).

A elevação da pressão parcial de CO_2 no sangue arterial ($PaCO_2$), chamada hipercapnia, ocorre devido à hematose alveolar insuficiente em pacientes com doenças pulmonares e, em asmáticos, reflete condições mais graves da doença (Masuda et al., 2014; Mazzeo et al., 2004; Mutlu et al., 2002). Nesse contexto, cerca de 10 a 26% dos casos de asma ocorrem com hipercapnia, que está associada à instituição de ventilação mecânica e a altas taxas de mortalidade (Gupta et al., 2004; Scala, 2010; Stow et al., 2007). De maneira semelhante, a hipoxemia é comum em exacerbações agudas devido ao

estreitamento das vias aéreas e ao acúmulo de muco, que impedem a troca gasosa adequada (Caplan e Hamzaoui, 2023). Ainda foi recentemente associada à piora da asma noturna (Sundbom et al., 2022).

A hipersensibilidade ao CO_2 e à hipóxia pode ter implicações relevantes na asma, uma vez que a prevalência de comorbidades associadas à instabilidade do sistema quimiorreflexo é consideravelmente maior na população asmática, com destaque para o transtorno de pânico (TP) e a apneia obstrutiva do sono (AOS) (Favreau et al., 2014; Goodwin et al., 2010; Kong et al., 2017). Estudos clássicos demonstram que indivíduos com TP apresentam hipersensibilidade ao CO_2 (Klein, 1993). De maneira semelhante, na AOS, episódios recorrentes de hipóxia durante o sono levam à sensibilização dos quimiorreceptores periféricos, tornando-os mais reativos (Prabhakar et al., 2023). Dessa forma, a inflamação alérgica observada na asma, bem como os quadros de hipoxemia e/ou hipercapnia durante crises graves, poderiam desestabilizar o sistema de controle ventilatório, favorecendo a ocorrência de comorbidades e potencializando a gravidade clínica da doença.

Em estudos com humanos, a resposta quimiorreflexa permanece controversa e confusa em indivíduos asmáticos. No entanto, estudos em modelos animais reforçam a evidência de que o corpo carotídeo é ativado pela exposição a alérgenos, por meio de mediadores inflamatórios circulantes, como IL-4, IL-5 e IL-13, que aumentam a sinalização aferente do quimiorreceptor (Jendzjowsky et al., 2021; Katayama et al., 2022). Nesse contexto, investigar as consequências da asma no sistema quimiorreflexo é fundamental para elucidar a heterogeneidade clínica da doença e aprimorar o manejo do paciente, uma vez que a disfunção desse sistema pode agravar sintomas, favorecer exacerbações e predispor ao desenvolvimento de comorbidades.

2. OBJETIVO

Em vista das evidências expostas, o primeiro objetivo desta pesquisa foi avaliar os padrões ventilatório e metabólico basal e pós-desafio respiratório em camundongos machos e fêmeas desafiados com o ácaro da poeira doméstica (HDM). Como segundo objetivo, foi proposto avaliar a resposta ventilatória e

metabólica de camundongos machos e fêmeas sensibilizados com o HDM durante a exposição à hipercapnia 7% e à hipóxia 7%.

3. REVISÃO DE LITERATURA

3.1. ASMA ALÉRGICA

3.1.1. Definição, epidemiologia e patogenia

A asma é uma condição crônica, complexa e heterogênea, caracterizada por inflamação das vias aéreas, que desencadeia processos como a produção de muco, o remodelamento e a hiperresponsividade brônquica (GINA, 2020). Em 2019, foi estimado que cerca de 262 milhões de pessoas eram acometidas pela asma em todo o mundo, o que resultou em 461.000 mortes, segundo o estudo Global Burden of Disease (IHME, 2024). A prevalência varia em função da idade e do sexo, sendo mais comum em meninos na infância, enquanto, na idade adulta, as mulheres se tornam mais afetadas, sugerindo que os hormônios sexuais desempenham um papel de destaque na manifestação dessa doença (Cephus et al., 2017; Dharmage et al., 2019; Stern et al., 2020).

Dada sua heterogeneidade, a asma pode ser classificada em diferentes fenótipos e endótipos, que refletem variações na manifestação clínica, nos mecanismos inflamatórios e na resposta ao tratamento (Akar-Ghibril et al., 2020). Do ponto de vista fenotípico, a asma pode ser classificada em alérgica (asma início na infância) ou não alérgica (asma de início tardio) (Akar-Ghibril et al., 2020). A asma alérgica ou de início na infância é o fenótipo mais comum e está associada a outras condições inflamatórias, como dermatite e rinite (Schatz e Rosenwasser, 2014). A asma de início tardio é geralmente mais grave e menos associada à alergia (Hammad e Lambrecht, 2021).

A asma alérgica está associada à resposta de células T auxiliares do tipo 2 (Th2) devido ao contato precoce com alérgenos ambientais, como ácaros da poeira doméstica (HDM), pólen e barata. As células epiteliais pulmonares reconhecem antígenos e produzem IL-33, IL-25 e IL-7, que ativam células dendríticas e células linfoides inatas do grupo 2. Estas, por sua vez, estimulam a diferenciação dos linfócitos Th2 e a produção de citocinas do tipo 2, incluindo

IL-4, IL-5 e IL-13. A IL-4 estimula a produção de imunoglobulinas do tipo E (IgE) antígeno-específicas pelos linfócitos B. A IgE, por sua vez, é necessária para induzir a degranulação de mastócitos, com liberação de novos mediadores inflamatórios responsáveis pela fase inicial da patogenia. A IL-5 é a principal citocina envolvida na regulação dos eosinófilos, controlando sua diferenciação, ativação e sobrevivência. A eosinofilia das vias aéreas é um dos principais fatores associados ao aumento da espessura da musculatura lisa, decorrente da produção de TGF-β. A IL-13 também estimula a produção de muco pelas células caliciformes e contribui para o remodelamento das vias aéreas. Em conjunto, essas citocinas formam um eixo integrado da imunidade do tipo 2 (Hammad e Lambrecht, 2021).

A fase tardia da asma alérgica culmina em alterações morfofuncionais das vias aéreas, caracterizadas por aumento da espessura da membrana basal, hipertrofia da musculatura lisa e danos epiteliais. Estas alterações contribuem para episódios reversíveis de declínio da função pulmonar (Biselli et al., 2022), evidenciado pela redução do volume expiratório forçado (VEF_1) no teste de espirometria (Fuhlbrigge et al., 2001; Hesselink et al., 2006; Kitch et al., 2004). Vale ressaltar que este indicador pode permanecer inalterado em pacientes com o fenótipo alérgico da doença, dependendo de fatores como sexo, VEF_1 basal, reversibilidade e duração da doença, e da variabilidade do VEF_1 (Bucchieri et al., 2021; Cibella et al., 2002; Lampalo et al., 2018; Sears et al., 2007; Soremekun et al., 2023). Dessa forma, a piora da função pulmonar na asma, quando presente, indica um efeito deletério do processo inflamatório sobre a capacidade de troca gasosa pulmonar.

Adicionalmente, as células epiteliais das vias aéreas expostas a alérgenos aumentam a geração de espécies reativas de oxigênio (EROs), levando à apoptose e lesão do epitélio das vias aéreas (Sauler et al., 2019; James et al., 2021). Evidências crescentes revelaram que a produção excessiva de EROs está fortemente correlacionada com a disfunção mitocondrial em condições alérgicas (Zuo e Wijegunawardana, 2021). De fato, alterações e disfunções mitocondriais foram observadas no epitélio e no músculo liso das vias aéreas de pacientes com asma e em modelos de asma alérgica em camundongos (Henricks e Nijkamp, 2001; Mabalirajan et al., 2008). Proteínas mitocondriais

danificadas levam à geração sustentada de EROs, que contribuem para a hiperresponsividade brônquica e podem ser um fator de risco para o desenvolvimento de asma em indivíduos suscetíveis (Aguilera-Aguirre et al., 2009).

3.1.2. Diferenças sexuais na manifestação da asma

Na infância, a asma alérgica é mais prevalente em meninos, mas, após a puberdade, as mulheres apresentam maior risco de desenvolver o tipo não alérgico, que possui menor associação com alergia e maior resistência à terapia com corticosteroides (De Marco et al., 2000). As variações na ocorrência de asma ao longo da vida coincidem com as flutuações nos níveis de hormônios sexuais, sugerindo fortemente sua participação na patogênese da doença (Cephus et al., 2017; Dharmage et al., 2019; Stern et al., 2020).

Nesse contexto, a testosterona foi considerada protetora em pacientes asmáticos, contribuindo para a manutenção do equilíbrio entre a imunidade autoimune e a imunidade protetora (Canguven & Albayrak, 2011). De fato, observou-se que pacientes do sexo masculino com asma moderada ou grave apresentavam níveis reduzidos de testosterona, enquanto aqueles com a forma leve da doença mantinham concentrações hormonais dentro da normalidade (Mileva e Maleeva, 1988). Em paralelo, os estrogênios foram associados a um perfil pró-inflamatório, especialmente à via de sinalização mediada pelo receptor de estrogênio alfa (ER-α). No entanto, a ativação do ER-β foi associada à menor hiperresponsividade brônquica e eosinofilia, sugerindo que o perfil pró-facilitador do estradiol na asma não é absoluto (Ambhore et al., 2019; Fuseini et al., 2017; Yung et al., 2018).

Além disso, Newcomb et al. (2015) relataram maiores concentrações de IL-17A em mulheres asmáticas em comparação com homens. A IL-17A é uma citocina pró-inflamatória associada ao fenótipo não alérgico mais grave da asma. No mesmo estudo, modelos murinos intactos de ambos os sexos e fêmeas ovariectomizadas (OVX) submetidas à reposição hormonal com estradiol combinado com progesterona (E_2+P) e testosterona, foram avaliados quanto aos níveis de IL-17A. Observou-se que as fêmeas OVX suplementadas com E_2+P apresentaram níveis mais elevados de IL-17A, enquanto os animais que

receberam testosterona apresentaram os níveis mais baixos. Esses achados sugerem que os hormônios sexuais femininos podem contribuir para um fenótipo da doença menos alérgico e mais grave.

De forma consistente, estudos indicam aumento da incidência de asma em mulheres na pós-menopausa submetidas à terapia de reposição hormonal. Por exemplo, Troisi et al. (1995), em um seguimento de 10 anos envolvendo 184 mulheres com idades entre 34 e 68 anos, observaram uma associação entre a terapia com estradiol e o aumento da incidência de asma. Achados semelhantes foram relatados por outros autores, que demonstraram maior taxa de diagnóstico recente de asma em mulheres na pós-menopausa em uso de terapia hormonal (Romieu et al., 2010; Triebner et al., 2016), os quais foram corroborados por meta-análises e revisões sistemáticas (Zemp et al., 2012).

Em conjunto, essas evidências reforçam a participação dos hormônios sexuais na incidência, progressão e modulação da gravidade da asma ao longo da vida, bem como a necessidade de inclusão de ambos os sexos nas pesquisas pré-clínicas.

3.1.3. Modelo murino: Ácaro da poeira doméstica

Modelos murinos de asma induzida pela exposição ao ácaro da poeira doméstica (*house dust mite*, HDM) têm sido amplamente utilizados devido à elevada relevância translacional para a asma alérgica, uma vez que o HDM é um agente causal natural da doença em humanos (Aun et al., 2017). Nesse modelo, a administração do extrato de HDM em roedores é capaz de mimetizar aspectos centrais da asma humana, incluindo inflamação eosinofílica, produção de IgE antígeno-específica, hiperresponsividade e remodelamento das vias aéreas (Carrol et al., 2023). No entanto, vale salientar que a intensidade, ou mesmo a presença, dessas respostas varia em função do protocolo experimental, incluindo a dose, a frequência e a duração da exposição ao HDM (Carrol et al., 2023). Embora as alterações estruturais sejam mais facilmente induzidas em camundongos da linhagem BALb/c, os C57Bl/6 também respondem satisfatoriamente ao alérgeno (Woodrow et al., 2023).

Nesse contexto, um estudo recente identificou alterações em diversos parâmetros respiratórios de camundongos C57Bl/6 e BALb/c sensibilizados com

HDM por meio de pletismografia de dupla câmara (Boucher et al., 2021). Neste estudo, a inflamação pulmonar decorrente do HDM resultou em menor volume corrente e menor ventilação minuto em ambas as linhagens (Boucher et al., 2021). Ainda, camundongos C57Bl/6 apresentaram maior resistência das vias aéreas e menor fluxo expiratório médio, embora de forma mais sutil em comparação aos animais BALb/c (Boucher et al., 2021). Tais alterações refletem com precisão os quadros obstrutivos observados em indivíduos asmáticos, evidenciando que o HDM é um modelo valioso para o estudo da asma em pesquisas translacionais.

Em relação à ativação imunológica, a exposição ao HDM promove um perfil inflamatório predominantemente do tipo 2, com aumento das citocinas IL-4, IL-5 e IL-13, bem como da liberação de citocinas epiteliais como IL-33 e IL-25, que contribuem para a amplificação da resposta inflamatória (Gregory e Lloyd, 2011). Embora a linhagem BALb/c reproduza de forma mais fiel as características marcantes da asma alérgica, devido à predisposição à resposta do tipo Th2, evidências crescentes indicam que camundongos C57Bl/6 desenvolvem uma resposta inflamatória robusta nas vias aéreas após exposição ao HDM (Allgire et al., 2023; Makino et al., 2021; Raemdonck et al., 2016).

3.2. QUIMIOSSENSIBILIDADE

3.2.1. Papel do sistema nervoso central e periférico

Respirar é um processo essencial para a obtenção de oxigênio (O_2) e a eliminação de dióxido de carbono (CO_2), mantendo o equilíbrio ácido-base nos tecidos. É um processo altamente regulado, que envolve a integração contínua entre sinais químicos e neurais (Del Negro et al., 2018). Células especializadas capazes de detectar alterações nas pressões parciais de O_2, CO_2 e pH no fluido ao seu redor são chamadas de quimiorreceptores (Heymans & Bouckaert, 1930; Loeschcke, 1982; Mitchell, 1963; Putnam et al., 2004; Nattie, 1999, 2000).

A quimiorrecepção periférica é mediada pelos corpos carotídeos, localizados na bifurcação da artéria carótida comum (Blain et al., 2010; Brinkman e Sharma, 2018). As células glômicas do tipo I do corpo carotídeo são altamente sensíveis à pressão parcial de oxigênio arterial (P_aO_2), à pressão parcial de CO_2 arterial (P_aCO2) e ao pH, sendo os principais sensores de oxigênio do corpo

(Pichard, 2015). A informação sensorial do corpo carotídeo é transmitida pelo ramo do seio carotídeo do nervo glossofaríngeo até o núcleo do trato solitário (NTS) no bulbo, onde ocorre a integração do sinal aferente com o centro controlador da respiração bulbar, permitindo uma rápida resposta compensatória à hipoxemia (Li e Nattie, 2006; Takakura et al., 2006; Guner et al., 2008).

A ventilação também é controlada por quimiorreceptores centrais, que respondem a alterações na relação CO_2/pH. A hipercapnia (aumento da $PaCO_2$) implica na elevação da concentração de íons H^+ e na acidificação do líquor cefalorraquidiano, que são detectadas por neurônios sensíveis ao CO_2/H^+ e por células da glia. (Guyenet et al., 2010). Múltiplos sítios no sistema nervoso central (SNC) participam da quimiorrecepção e acionam respostas autonômicas que resultam no aumento da ventilação, a fim de normalizar a P_aCO_2 (Nattie e Li, 2012; Gargaglioni et al., 2010). Neurônios quimiossensíveis podem ser encontrados no hipotálamo lateral, no núcleo fastigial do cerebelo, no locus coeruleus (LC), no núcleo retrotrapezoide (RTN), no núcleo caudal da rafe bulbar e no núcleo do trato solitário (NTS) (Biancardi et al., 2008; Conrad et al., 2009; Ritucci et al., 2005; Wang et al., 1998; Ziemann et al., 2009; Gargaglioni et al., 2010).

Portanto, a quimiossensibilidade constitui um mecanismo fundamental para a adaptação respiratória em condições de hipoxemia e/ou hipercapnia. Dessa forma, a atividade alterada destes núcleos pode predispor a certas condições patológicas, como transtorno do pânico, apneia obstrutiva do sono e síndrome de Rett (Bailey et al., 2003, Griez and Schruers, 2003; Kamra et al., 2025; Taneja et al., 2009).

3.2.2. Instabilidade em pacientes asmáticos e achados em modelos animais

Na asma, o estímulo ventilatório desempenha papel fundamental na determinação da gravidade da doença e pode ser influenciado por diversos fatores, como quimiossensibilidade, tensão arterial basal de oxigênio ou dióxido de carbono, impedância mecânica e disfunção da musculatura respiratória (Hida, 1999). Em asmáticos, a hipoxemia isolada é considerada um estímulo leve à respiração, mas a presença de hipercapnia pode potencializar seu efeito nas áreas centrais envolvidas no controle respiratório (Town e Allan, 1989).

No entanto, a resposta quimiorreflexa em indivíduos asmáticos permanece controversa e confusa. Alguns estudos em humanos evidenciaram uma resposta normal à hipóxia e à hipercapnia em pacientes asmáticos (Cosgrove et al., 1976 ; Kelsen et al., 1979). No entanto, Hutchison e Olinsky (1981) relataram que um adulto jovem com asma grave apresentou baixa resposta à hipercapnia. Ainda no mesmo estudo, três crianças asmáticas apresentaram resposta atenuada à hipóxia, mas responderam normalmente à hipercapnia (Hutchison e Olinsky, 1981). Em três outros estudos, a resposta ventilatória à hipercapnia mostrou-se aumentada no grupo asmático (Munakata et al., 1993; Tandon, 1969; Rebuck e Read, 1971). Por fim, em pacientes com histórico de asma quase fatal, relatou-se menor resposta ventilatória à hipóxia em comparação com pacientes com asma controlada ou com indivíduos saudáveis (Gibson, 1995; Hudgel e Weil, 1975; Hutchison e Olinsky, 1981; Kikuchi et al., 1994; Smith e Hudgel, 1980).

Embora informações conflitantes tenham sido relatadas em pacientes humanos, evidências recentes reforçam a ideia de que o corpo carotídeo desempenha um papel ativo na fisiopatologia da asma, participando do reflexo de broncoconstrição induzido pela exposição a alérgenos em modelos experimentais de asma (Jendzjowsky et al., 2018). Nesse contexto, demonstrou-se que as células glômicas do corpo carotídeo podem funcionar como um imunossensor, ao aumentarem a sinalização aferente em resposta à sensibilização por mediadores inflamatórios sistêmicos (Jendzjowsky et al., 2021; Katayama et al., 2022). Esses achados evidenciam a participação do corpo carotídeo na hiperresponsividade das vias aéreas; contudo, não comprovam o aumento da estimulação ventilatória.

Nesse contexto, apenas dois estudos investigaram as consequências da inflamação pulmonar sobre o quimiorreflexo. Em ratos machos sensibilizados com ovalbumina (OVA), a resposta ventilatória hipóxica foi aumentada, sugerindo maior sensibilidade do corpo carotídeo decorrente da inflamação (Morgan et al., 2024). Em contrapartida, o tratamento com OVA em cobaias machos atenuou o quimiorreflexo hipóxico (Xu et al., 2005). Ainda neste estudo, a resposta ventilatória à hipóxia manteve-se diminuída em até 74% mesmo após a administração de doxapram (estimulante dos quimiorreceptores carotídeos).

Apesar de a OVA induzir um quadro inflamatório semelhante ao da asma no pulmão de roedores, não é capaz de induzi-lo em seres humanos (Aun et al., 2017), sendo interessante avaliar se o HDM é capaz de alterar o quimiorreflexo. Nesse contexto, camundongos desafiados com HDM apresentaram aumento na expressão de proteína c-Fos em neurônios noradrenérgicos do NTS, sugerindo que a inflamação das vias aéreas pode sensibilizar circuitos neurais quimiossensíveis (Su et al., 2024).

Adicionalmente, a alta prevalência de comorbidades como apneia obstrutiva do sono (AOS) e transtorno de pânico (TP) na população asmática fortalece a hipótese de que a inflamação alérgica das vias aéreas pode alterar a quimiossensibilidade (Cooper et al., 2007; Favreau et al., 2014; Goodwin et al., 2010; Hasler et al., 2005; Kong et al., 2019; Lavoie et al., 2005; Teodorescu et al., 2015). A AOS é uma condição prevalente em indivíduos do sexo masculino e tipicamente associada à maior quimiossensibilidade periférica, enquanto o TP está relacionado ao aumento da sensibilidade ao CO_2 e é cerca de duas vezes mais prevalente em mulheres do que em homens (Dempsey e Gibbons, 2024; Klein, 1993; Vollmer et al., 2016; Wang et al., 2007; Wemmie, 2011). Assim, é possível que a asma compartilhe mecanismos fisiopatológicos com essas condições, incluindo alterações na sensibilidade dos quimiorreceptores de maneira sexo-específica.

4. REFERÊNCIAS

Agache I, et al. Asthma phenotypes and endotypes. Allergy, 67:835-846, 2012.

Aguilera-Aguirre L, et al. Mitochondrial dysfunction in asthma. J Immunol, 183:5379-5387, 2009.

Aun MV, et al. Animal models of asthma. J Asthma Allergy, 10:293-301, 2017.

Bailey JE, Argyropoulos SV, Lightman SL, Nutt DJ. Does the brain noradrenaline network mediate CO2 challenge effects? J Psychopharmacol, 17(3):252-259, 2003.

Biancardi V, et al. Locus coeruleus noradrenergic neurons and CO2 drive to breathing. Pflugers Arch, 455(6):1119-1128, 2008.

Biselli PJC, et al. Lung mechanics evolution. Front Physiol, 13:817263, 2022.

Blain GM, Smith CA, Henderson KS, Dempsey JA. Peripheral chemoreceptors determine the respiratory sensitivity of central chemoreceptors to CO2. J Physiol, 588:2455-2471, 2010.

Brinkman JE, Sharma S. Physiology, respiratory drive. In: StatPearls. Treasure Island (FL): StatPearls Publishing, 2018.

Bucchieri S, et al. Lung function decline in asthma. Diagnostics (Basel), 11:1637, 2021.

Canguven O, Albayrak S. Testosterone and asthma hypothesis. Med Hypotheses, 76:585-588, 2011.

Caplan M, Hamzaoui O. Cardio-respiratory interactions in asthma. Front Physiol, 14:1232345, 2023.

Carroll OR, et al. Respiratory physiology in asthma models. Front Physiol, 14:1099719, 2023.

Cephus JY, et al. Testosterone and ILC2s. Cell Rep, 21:2487-2499, 2017.

Cibella F, et al. Lung function decline. Chest, 122:1944-1948, 2002.

Conrad SC, et al. Development of chemosensitivity in neurons from the nucleus tractus solitarii. Respir Physiol Neurobiol, 166:4-12, 2009.

Cooper CL, et al. Anxiety and asthma. BMC Fam Pract, 8:62, 2007.

Cosgrove JF, et al. Ventilatory response to CO2 in asthmatic children. Pediatrics, 57(6):952-959, 1976.

De Marco R, et al. Sex differences in asthma incidence. Am J Respir Crit Care Med, 162:68-74, 2000.

Del Negro, C. A., Funk, G. D., & Feldman, J. L.. Breathing matters. Nature Reviews Neuroscience, 19(6):351-367, 2018.

Dempsey JA, Gibbons TD. O2, CO2 and breathing. J Physiol, 602(21):5571-5585, 2024.

Dharmage SC, et al. Asthma epidemiology. Front Pediatr, 7:1-15, 2019.

Favreau H, et al. Panic disorder and asthma control. Psychosom Med, 76(2):147-155, 2014.

Fuhlbrigge AL, et al. FEV1 and asthma attacks. J Allergy Clin Immunol, 107:61-67, 2001.

Gargaglioni LH, et al. The locus coeruleus and central chemosensitivity. Respir Physiol Neurobiol, 173(3):264-273, 2010.

Gibson GJ. Perception and respiratory control in asthma. Thorax, 50(Suppl 1):S2-S4, 1995.

Global Initiative for Asthma (GINA). Global Strategy for Asthma Management and Prevention, 2020.

Goodwin RD, et al. Asthma and mental disorders. J Psychosom Res, 68(2):165-173, 2010.

Gregory LG, Lloyd CM. HDM allergy mechanisms. Trends Immunol, 32(9):402-411, 2011.

Griez E, Schruers K. Mechanisms of CO2 challenges. J Psychopharmacol, 17(3):267-268, 2003.

Guner I, et al. Intracerebroventricular serotonin reduces the degree of acute hypoxic ventilatory depression in peripherally chemodenervated rabbits. Chin J Physiol, 51:136-145, 2008.

Gupta D, et al. ICU asthma outcomes. Crit Care, 8:R112, 2004.

Hammad H, Lambrecht BN. Immunology of asthma. Cell, 184:1469-1485, 2021.

Hasler G, et al. Asthma and panic. Am J Respir Crit Care Med, 171(11):1224-1230, 2005.

Henricks PA, Nijkamp FP. ROS in asthma. Pulm Pharmacol Ther, 14:409-420, 2001.

Hernandez-Miranda LR, Birchmeier C. CO2 in the spotlight. eLife, 4:e08086, 2015.

Hesselink AE, et al. Pulmonary function and QoL. J Asthma, 43:513-519, 2006.

Heymans C, Bouckaert JJ. Sinus caroticus and respiratory reflexes. Cerebral blood flow and respiration. Adrenaline apnoea. J Physiol, 69:13-14, 1930.

Hida W. Papel do estímulo ventilatório na asma e na doença pulmonar obstrutiva crônica. Curr Opin Pulm Med, 5(6):339, 1999.

Hida W. Role of ventilatory drive in asthma and COPD. Curr Opin Pulm Med, 5(6):339, 1999.

Hudgel DW, Weil JV. Depression of ventilatory drives in severe asthma. Chest, 68(4):493-497, 1975.

Hutchison AA, Olinsky A. Hypoxic and hypercapnic response in asthma. Thorax, 36(10):759-763, 1981.

IHME. Global Burden of Disease Study 2021, 2024.

Ikeda K, Kawakami K, Onimaru H, Okada Y, Yokota S, Koshiya N, et al. The respiratory control mechanisms in the brainstem and spinal cord: integrative views of the neuroanatomy and neurophysiology. J Physiol Sci, 67(1):45-62, 2017.

James BN, et al. Ceramide in asthma. J Allergy Clin Immunol, 147:1936-1948, 2021.

Jendzjowsky NG, et al. Carotid body signaling in asthma. Nat Commun, 9:4030, 2018.

Jendzjowsky NG, Roy A, Wilson RJ. Carotid bodies sensitized by allergen exposure. J Neuroinflammation, 18:191, 2021.

Kamra K, Xia Z, Zucker IH, Schultz H, Wang HJ. Chemoreflex function in pulmonary diseases - A review. J Physiol, 603(16):4461-4482, 2025.

Katayama PL, et al. Carotid body detects TNF-alpha. Brain Behav Immun, 102:370-386, 2022.

Kelsen S, Fleegler B, Altose M. Respiratory neuromuscular response in asthma. Am Rev Respir Dis, 120:517-527, 1979.

Kikuchi Y, et al. Chemosensitivity in near-fatal asthma. N Engl J Med, 330(19):1329-1334, 1994.

Kitch BT, et al. FEV1 and asthma risk. Chest, 126:1875-1882, 2004.

Klein DF. CO2 hypersensitivity and panic. Arch Gen Psychiatry, 50(1):306-317, 1993.

Kong DL, et al. OSA and asthma meta-analysis. Sci Rep, 7:4088, 2017.

Lampalo M, et al. Biomarkers in asthma phenotypes. Acta Clin Croat, 57:96-102, 2018.

Lavoie KL, et al. Psychiatric disorders and asthma control. Respir Med, 99(10):1249-1257, 2005.

Li A, Nattie EE. Catecholamine neurons in rats modulate sleep, breathing. 2006.

Mabalirajan U, et al. Mitochondrial dysfunction in asthma. J Immunol, 181:3540-3548, 2008.

Masuda Y, et al. Hypercapnia in asthma. J Anesth, 28:610-612, 2014.

Mazzeo AT, et al. Severe asthma and hypercapnia. Paediatr Anaesth, 14:596-603, 2004.

Mileva Z, Maleeva A. Testosterone in asthma. Vutr Boles, 27:29-32, 1988.

Mitchell RA, Loeschcke HH, Massion WH, Severinghaus JW. Respiratory responses mediated through superficial chemosenitive areas on the medulla. J Appl Physiol,18:523-533, 1963.

Morgan BJ, et al. Altered breathing control in allergic airway inflammation. J Neurophysiol, 132(5):1650-1666, 2024.

Munakata M, et al. Female asthmatics and hypercapnic chemosensitivity. Chest, 104(6):1718-1722, 1993.

Mutlu GM, et al. Permissive hypercapnia in asthma. Crit Care Med, 30:477-480, 2002.

Nattie E. CO2, brainstem chemoreceptors and breathing. Prog Neurobio, 59:299-331, 1999.

Nattie E. Multiple sites for central chemoreception: their roles in response sensitivity and in sleep and wakefulness. Respir Physiol, 122:223-235, 2000.

Nattie E, Li A. Central chemoreceptors: locations and functions. In: Comprehensive Physiology, 221-254, 2012.

Newcomb DC, et al. Sex hormones and IL-17A in asthma. J Allergy Clin Immunol, 136, 2015.

Pichard LE, et al. Role of BK channels in murine carotid body neural responses in vivo. Adv Exp Med Biol, 860:325-333, 2015.

Prabhakar NR, Peng YJ, Nanduri J. Carotid body hypoxia sensing. J Physiol, 601(24):5481-5494, 2023.

Putnam RW, Filosa JA, Ritucci NA. Cellular mechanisms involved in CO2 and acid signaling in chemosensitive neurons. Am J Physiol Cell Physiol, 287:C1493-C1526, 2004.

Rebuck AS, Read J. Ventilatory response patterns in severe asthma. Clin Sci, 41(1):13-21, 1971.

Ritucci NA, et al. Response of membrane potential and intracellular pH to hypercapnia. Am J Physiol Regul Integr Comp Physiol, 289:R851-R861, 2005.

Romieu I, et al. Hormone therapy and asthma. Thorax, 65:292-297, 2010.

Sauler M, et al. Cell death in lung. Annu Rev Physiol, 81:375-402, 2019.

Scala R. Noninvasive ventilation in asthma. Respir Care, 55:630-637, 2010.

Schatz M, Rosenwasser L. Allergic asthma phenotype. J Allergy Clin Immunol Pract, 2:645-648, 2014.

Sears MR. Lung function decline in asthma. Eur Respir J, 30:411-413, 2007.

Smith TF, Hudgel DW. Hypoxic ventilatory response in asthmatic children. J Pediatr, 97(5):736-741, 1980.

Soremekun S, et al. Exacerbations and lung function decline. Thorax, 78:643-652, 2023.

Stern J, et al. Asthma epidemiology. Semin Immunopathol, 42:5-15, 2020.

Stow PJ, et al. ICU outcomes in asthma. Crit Care, 2007.

Su Y, et al. Brainstem neurons control allergen-induced airway hyperreactivity. Nature, 631(8021):601-609, 2024.

Sundbom F, et al. Asthma and asthma-related comorbidity: effects on nocturnal oxygen saturation. J Clin Sleep Med, 18(11), p. 2635-2641, 2022.

Takakura AC, et al. Peripheral chemoreceptor inputs to retrotrapezoid nucleus (RTN) CO2-sensitive neurons in rats. J Physiol, 572:503-523, 2006.

Taneja P, Ogier M, Brooks-Harris G, Schmid DA, Katz DM, Nelson SB. Pathophysiology of locus coeruleus neurons in Rett syndrome. J Neurosci, 29(39):12187-12195, 2009.

Teodorescu M, et al. Asthma and OSA association. JAMA, 313(2):156-164, 2015.

Town G, Allan C. Ventilatory responses to hypoxia and hypercapnia in asthmatics. Aust N Z J Med, 19(5):426-430, 1989.

Triebner K, et al. Menopause and asthma onset. J Allergy Clin Immunol, 2016.

Troisi RJ, et al. Estrogen and asthma risk. Am J Respir Crit Care Med, 152:1183-1188, 1995.

Vollmer LL, et al. CO2 and fear circuits. Biol Psychiatry, 80(7):541-551, 2016.

Wang D, et al. Hypercapnic response and OSA. Sleep Breath, 11:103-108, 2007.

Wang D, et al. Ventilatory response to hypercapnia and OSA. Sleep Breath, 11(2):103-108, 2007.

Wang W, et al. Chemosensitivity of rat medullary raphe neurons in culture. J Physiol, 511(2):433-450, 1998.

Wemmie JA. Amygdala CO2 sensing. Behav Brain Res, 377:112236, 2019.

Woodrow JS, et al. Animal models of asthma. Cells, 12(7):1091, 2023.

Xu F, et al. Ovalbumin alters ventilatory responses. J Appl Physiol, 99(5):1782-1788, 2005.

Zemp E, et al. Asthma and menopause. Maturitas, 73:212-217, 2012.

Ziemann AE, et al. The amygdala detects CO2 and acidosis to elicit fear. Cell, 139(5):1012-1021, 2009.

Zuo L, Wijegunawardana D. ROS and lung disease. Adv Exp Med Biol, 1304:187-204, 2021.

CAPÍTULO 2 – ARTICLE

Allergic Airway Inflammation Induces Sex-Specific Alterations In Chemoreflex Function And Metabolism In C57Bl/6 Mice

Abstract – Allergic asthma is a chronic inflammatory disease of the airways. Growing evidence suggests that asthma-associated inflammation may destabilize the respiratory control system, thereby promoting comorbidities and worsening disease progression. In this context, the present study aimed to investigate central and peripheral chemosensitivity in a murine model of allergic airway inflammation. For this purpose, male and female C57BL/6 mice were exposed to house dust mites (HDMs), and their ventilatory and metabolic patterns were assessed under room air, hypoxia (7% O_2), and hypercapnia (7% CO_2). HDM exposure induced sex-specific alterations in ventilatory patterns under room-air conditions, with an increase in respiratory frequency (f_R) in males, whereas females exhibited a reduction in basal metabolic rate, as evidenced by decreased oxygen consumption (VO_2). During hypoxia, HDM-exposed males showed an enhanced ventilatory response, characterized by increased f_R, minute ventilation (V_E), and ventilatory equivalent for O_2 (V_E/VO_2), whereas females displayed a blunted response, with increased VO_2 and decreased V_E/VO_2. Under hypercapnic conditions, HDM-exposed males exhibited a reduced ventilatory response, with increased VO_2 and decreased V_E/VO_2, whereas females showed increased VO_2 without changes in V_E/VO_2. Taken together, our findings suggest that HDM-induced allergic inflammation promotes sex-dependent alterations in basal metabolism and differentially modulates peripheral and central chemosensory responses.

Keywords: allergic inflammation, chemoreflex, hypercapnia, hypoxia.

1. INTRODUCTION

Asthma is a chronic inflammatory disease of the airways, characterized by structural changes that lead to airflow obstruction and hyperresponsiveness (GINA, 2020). In 2019, an estimated 262 million people worldwide were affected by the disease, which was responsible for 461,000 deaths, according to the Global Burden of Disease study (IHME, 2024). Prevalence varies according to age and sex, being more common in boys during childhood, whereas women are more affected in adulthood, suggesting that sex hormones play an important role in disease manifestation (Cephus et al., 2017; Dharmage et al., 2019; Stern et al., 2020).

Given the heterogeneity of clinical manifestations, asthma can be classified into allergic and non-allergic phenotypes (Hammad and Lambrecht, 2021). Allergic asthma is the most common phenotype and typically begins in

childhood (Levy et al., 2023). Its pathogenesis is characterized by the activation of T helper type 2 (Th2) lymphocytes in response to sensitization by environmental allergens such as house dust mites, pollen, and animal dander (Hammad and Lambrecht, 2021). Clinical symptoms arise from an inflammatory response, mainly mediated by interleukins (IL)-4, IL-5, and IL-13, which play central roles in the allergic cascade (Hammad and Lambrecht, 2021). Collectively, these mechanisms lead to airway remodeling, including mucus accumulation and smooth muscle hypertrophy and hyperplasia, resulting in reversible bronchoconstriction (Agache et al., 2012; Woodruff et al., 2009).

Elevated arterial carbon dioxide partial pressure ($PaCO_2$) results from impaired alveolar gas exchange in patients with pulmonary diseases and, in asthmatic individuals, reflects more severe disease (Masuda et al., 2014; Mazzeo et al., 2004; Mutlu et al., 2002). In this context, approximately 10–26% of asthma cases present with hypercapnia (Scala, 2010), which is associated with the need for mechanical ventilation and high mortality rates (Gupta et al., 2004; Stow et al., 2007). Similarly, hypoxemia is common in severe asthma exacerbations due to airway narrowing and mucus accumulation, which impair adequate gas exchange (Rahnama'i et al., 2006). Furthermore, hypoxemia has recently been associated with worsening nocturnal asthma symptoms (Sundbom et al., 2022).

Increased sensitivity to CO_2 and hypoxia may have important implications for asthma, given the high prevalence of comorbidities associated with chemoreflex instability in the asthmatic population, particularly panic disorder (PD) and obstructive sleep apnea (OSA) (Favreau et al., 2014; Goodwin et al., 2010; Kong et al., 2017). Classical studies have shown that individuals with PD are hypersensitive to CO_2 (Klein, 1993), and recent evidence highlights the role of the locus coeruleus, a chemosensitive nucleus, in mediating this response (de Oliveira et al., 2026). Similarly, in OSA, recurrent hypoxic episodes during sleep sensitize peripheral chemoreceptors, increasing their reactivity (Mansukhani et al., 2016). Importantly, both PD and OSA display pronounced sex differences in prevalence, with PD being approximately two- to fourfold more prevalent in women (Olaya et al., 2018; Valdes et al., 2021), whereas OSA predominantly affects men (Franklin and Lindberg, 2015; Lévy et al., 2015), suggesting that sex-

dependent mechanisms may contribute to the interaction between asthma, chemoreflex dysfunction, and these comorbidities.

In human studies, chemoreflex responses in asthma remain controversial and not fully understood. However, animal models provide evidence that the carotid body is activated by allergen exposure via circulating inflammatory mediators, including IL-4, IL-5, and IL-13, thereby enhancing afferent signaling from peripheral chemoreceptors (Jendzjowsky et al., 2021; Katayama et al., 2022). In this context, investigating the effects of asthma on the chemoreflex system is essential for better understanding of disease's clinical heterogeneity and improving patient management, as dysfunction of this system may worsen symptoms, facilitate exacerbations, and predispose to comorbidities.

2. METHODS

2.1. Animals

Unanesthetized adult male and female C57BL/6 mice (20–25 g; 11–12 weeks of age) were used in the experiments. Animals were housed in a temperature-controlled chamber at 26 ± 1°C (ALE 9902001; Alesco Ltda, Monte Mor, Brazil) with a 12:12-h light-dark cycle and fed *ad libitum*. All experimental procedures followed the National Council of Control in Animal Experimentation (CONCEA-MCT-Brazil) guidelines and were approved by the local Animal Care and Use Committee (protocol no.5022/2024).

2.2. Airway inflammation model

To induce an airway inflammatory condition, the house dust mite extract (HDM, *Dermatophagoides pteronyssinus*; Salute Vita, Sao Paulo, SP, Brazil) was used. On day 0, animals were sensitized by intratracheal administration of 50 µg in 50 µL of sterile saline (0.9% NaCl) under isoflurane anesthesia. After 7 days, the animals were challenged with 20 µg in 40 µL of vehicle on days 7, 8, 9, and 10. The control group received a vehicle. Experiments and sample collection were performed on day 13.

2.3. Surgical procedure

Animals underwent laparotomy on day 0 of the experimental protocol to implant a temperature sensor (APT12 PIT Tag; Biomark, Boise, ID, USA) to monitor body temperature during the experiments. Isoflurane was used for anesthesia (5% for induction and 2% for maintenance).

2.4. Bronchoalveolar lavage

Bronchoalveolar lavage fluid (BALF) was collected as previously described (Marchica et al., 2011). Animals were anesthetized with sodium thiopental and tracheostomized using a cannula (26G needle). Using a 1 mL syringe, 0.8 mL of cold sterile saline (0.9% NaCl) was slowly instilled, then aspirated to recover the BALF. Four consecutive lavages were performed per animal. The total recovered volume was centrifuged at 2,000 × g for 5 min at 4 °C. The supernatant was aliquoted and stored at −80 °C for cytokine analysis. The BALF pellet was resuspended in 200 µL of cold sterile saline (0.9% NaCl) for total and differential cell counts. Approximately 10 µL of the cell suspension was used for total cell counting. For this purpose, 10 µL of 0.4% Trypan Blue solution was added to the sample. Cell counting was performed using a Neubauer chamber under a standard light microscope. Blue-stained (non-viable) cells were excluded. For differential cell counts, cytospin smears were prepared and stained with Panotico Rapido (Laborclin, Pinhais, PR, Brazil). Cells were counted under a light microscope to determine the number of mononuclear cells, eosinophils, and neutrophils out of a total of 300 cells.

2.5. Cytokine ELISA assay

IL-4, IL-5, and IL-13 levels were quantified in BALF, the right lung lobe, and plasma using the ELISA MAX Deluxe Set Mouse IL-4 and IL-5 kits (BioLegend, San Diego, CA, USA) and the Mouse IL-13 Uncoated ELISA Kit (Invitrogen, Carlsbad, CA, USA), respectively. BALF was collected as described above. After BALF collection, the right lung lobe was removed, weighed, and stored at –80 ºC. For plasma collection, animals were decapitated, and trunk blood was collected. Approximately 2 mL of blood was obtained from each mouse using a glass funnel and an Eppendorf tube containing diluted heparin (0.15 mL of sodium heparin, 5000 IU/mL, in 3 mL of 0.9% NaCl). Plasma was separated by centrifugation at 3,000 rpm for 10 min at 4 °C and stored at −80 °C. Lungs were homogenized in

RPMI 1640 medium containing protease inhibitors and were cleared by centrifugation at 10,000 × g for 5 min before analysis by ELISA. Cytokine concentrations were determined by ELISA according to the manufacturer's instructions. Standard curves ranged from 2.344 to 118.915 pg/mL, 12.938 to 615.621 pg/mL, and 9.986 to 615.621 pg/mL for IL-4, IL-5, and IL-13, respectively. The assay sensitivities were 1.626 pg/mL for IL-4 and 6.335 pg/mL for both IL-5 and IL-13.

2.6. Lung histology

To assess lung inflammation, the left lung lobe was removed after BALF collection and fixed in 10% buffered formalin for 24 h. Subsequently, the tissue was dehydrated, cleared, and embedded in paraffin. Transverse tissue sections (3 μm thick) were obtained and stained with hematoxylin and eosin (H&E) and periodic acid–Schiff (PAS). Histopathological analysis was performed on airways with intact epithelium. Peribronchial and perivascular inflammation was assessed by quantifying the thickness of inflammatory cell infiltrates surrounding the airways and blood vessels and scored using the following scale: 0, no inflammatory cell infiltrate; 1, few scattered inflammatory cells; 2, one to two inflammatory cell layers; 3, three to four inflammatory cell layers; and 4, more than four inflammatory cell layers. Total lung inflammation was defined as the sum of peribronchial and perivascular scores. Mucus expression was assessed within the airway epithelium with PAS staining. The percentage of the PAS+ cells in the epithelial lining was quantified and expressed using the following scale: 0, no goblet cells; 1, <25%; 2, 25–50%; 3, 50–75%; 4, ≥75%.

2.7. Respiratory challenges

To evaluate the effect of pulmonary inflammation on central and peripheral chemosensitivity, animals were exposed to two respiratory challenges: (1) isocapnic hypoxia (10% O_2, 0% CO_2, balance N_2) and (2) normoxic hypercapnia (7% CO_2, 21% O_2, balance N_2). The hypercapnia gas mixture was purchased from White Martins Gases Industriais Ltda (Osasco, SP, Brazil), whereas the hypoxic gas mixture was generated using a gas mixer (GSM-3; CWE, Ardmore, PA, USA).

2.8. Ventilatory parameters assessment

Ventilation ($\dot{V}_E$) was measured by whole-body plethysmography in a closed system. Airflow was maintained at 0.5 L.min^{-1} using an air pump and monitored with a mass flow meter (GFM17; Aalborg Instruments, Orangeburg, NY, USA). For $\dot{V}_E$ measurements, airflow was interrupted, and the chamber was fully sealed for 2 min. Pressure oscillations due to temperature differences between inspired and expired air were recorded using a differential pressure transducer (Spirometer; ADInstruments, Sydney, NSW, Australia) and digitized on a computer equipped with data acquisition software (PowerLab; ADInstruments, Sydney, NSW, Australia). For each experiment, volume calibration was performed by injecting 0.2 mL of air into the chamber using a graduated syringe. $\dot{V}_E$ was calculated as the product of respiratory frequency (f_R) and tidal volume (V_T). f_R was obtained by analyzing the number of respiratory events per minute. V_T was calculated using Drorbaugh and Fenn's equation (1955):

$$V_T = [V_K \times (P_T / P_K) \times T_b \times (P_B - P_C)] / [T_b \times (P_B - P_C) - T_C \times (P_B - P_b)]$$

Where P_T is the pressure deflection associated with each V_T; P_K is the pressure deflection associated with the injection of the calibration volume (V_K); T_C is the temperature in the animal chamber; P_B is the barometric pressure in Jaboticabal, SP, Brazil (705 mmHg); P_C is the water vapor pressure in the animal chamber; T_b is the animal body temperature; and P_b is the water vapor pressure at T_b. P_C and P_b were calculated indirectly using a standard reference table (Dejours, 1981).

$\dot{V}_E$ and V_T are presented under BTPS conditions. Cycle duration (C_D), inspiration time (T_i), and expiration time (T_e) were also analyzed. The LabChart software (PowerLab System; ADInstruments/Chart Software, Sydney, NSW, Australia) was used for data analysis.

2.9. Metabolic and gas exchange measurements

Oxygen consumption ($\dot{V}O_2$) and CO_2 production ($\dot{V}CO_2$) were measured by indirect calorimetry using an open flow respirometry system in push mode. O_2 and CO_2 concentrations were monitored using gas analyzers (PA-10 and CA-10, respectively; Sable Systems International, North Las Vegas, NV, USA). The expired gas was dried over a small column of Drierite (Sigma-Aldrich, St. Louis,

MO, USA) before going through the analyzers. The air was continuously sampled, and data acquisition was performed using the PowerLab system (ADInstruments/Chart Software, Sydney, NSW, Australia). $\dot{V}O_2$ and $\dot{V}CO_2$ were calculated using the following equations (Lighton, 2008):

$$\dot{V}O_2 = FR_i [(F_iO_2 – F_eO_2) – F_eO_2 (F_eCO_2 – F_iCO_2)] / (1 – F_eO_2)$$

$$\dot{V}CO_2 = FR_i [(F_eCO_2 – F_iCO_2) – F_eCO_2 (F_iO_2 – F_eO_2)] / (1 – F_eCO_2)$$

Where FR_i is the inlet flow rate of air through the chamber; F_iO_2 is the inspired fraction of O_2; F_eO_2 is the expired fraction of O_2; F_iCO_2 is the inspired fraction of CO_2; and F_eCO_2 is the expired fraction of CO_2. $\dot{V}O_2$ and $\dot{V}CO_2$ were divided by the body mass and expressed in standard conditions (STPD).

Respiratory quotient (RQ) was calculated as the ratio of $\dot{V}CO_2$ to $\dot{V}O_2$. Ventilatory equivalent for O_2 ($\dot{V}_E/\dot{V}O_2$) was obtained from the $\dot{V}O_2$ and $\dot{V}_E$ data.

2.10. Study design

2.10.1. Animal model characterization

To determine the asthma pattern induced by HDM, a group of control and HDM-exposed animals was euthanized on day 13 for BALF and lung collection (Figure 1 – Experiment 1). Subsequently, total BALF cells were quantified, and the supernatant was collected for cytokine quantification. The right lung lobe was frozen for cytokine assessment, and the left lobe was fixed for histology. For plasma cytokine quantification, another group of control and HDM-exposed animals was euthanized on day 13 of the allergen exposure protocol for blood collection. The lungs were also collected for cytokine quantification (right lobe) and histology (left lobe) (Figure 1 – Experiment 2).

2.10.2. Plethysmography experiments

A group of control and HDM-exposed animals underwent whole-body plethysmography on day 13 of the allergen exposure protocol. Animals were weighed and placed in a plethysmographic chamber ventilated with room air (21% O_2, 0% CO_2, and balanced N_2) for a 1-hour habituation period. Subsequently, two baseline measurements of ventilation and metabolic rate were obtained at 10-minute intervals. The animals were then exposed to either

hypercapnia (7% CO_2, 21% O_2, and balanced N_2) or hypoxia (7% O_2, 0% CO_2, and balanced N_2) for 20 min, with measurements performed at 10 and 20 min after the onset of exposure. Following the respiratory challenge, the chamber was returned to room air conditions for a 1-hour recovery period, during which one recovery measurement was obtained. Finally, the animals were subjected to the second respiratory challenge for an additional 20 min, and two further measurements were collected at 10-minute intervals. The order of the respiratory challenge exposure was performed randomly (Figure 1 – Experiment 3). At the end of the experiments, BALF and right and left lung lobes were collected for the analyses described in protocol 2.10.1.

2.11. Data analysis

Statistical analyses were performed using R software. For differential BALF cell counts, comparisons between groups were performed using the Student's t-test when data met normality assumptions. Total BALF cell counts and cytokine measurements were analyzed using two-way ANOVA, considering sex (male vs. female) and treatment (control vs. HDM) as independent factors. Data normality and homogeneity of variances were assessed using the Shapiro–Wilk and Levene tests, respectively. When the assumptions for parametric analysis were not met, a nonparametric Aligned Rank Transform (ART) ANOVA (ANOVA on ranks) was applied. For plethysmography experiments, two-way repeated measures ANOVA was used to evaluate the effects of treatment (HDM vs. control), time (baseline vs. recovery or 10 vs. 20 min), and their interaction, followed by appropriate post hoc comparisons. When parametric assumptions were violated, a repeated measures ANOVA on ranks was performed. Variables that differed under room-air conditions were expressed as delta values during hypoxic and hypercapnic exposures. Results were considered statistically significant when $p < 0.05$.

3. RESULTS

3.1. Characterization of the airway inflammation model

For total BALF cell counts, the Two-Way ANOVA showed a significant effect of HDM treatment, with no effect of sex or interaction between factors (treatment: $F(1,9) = 154.1872$, $p < 0.0001$; sex: $F(1,9) = 1.7378$, ns; treatment × sex: $F(1,9) = 0.1488$, ns). Post hoc analysis showed that total BALF cell counts were higher in HDM-treated female and male mice compared to their respective control groups (female: $p < 0.0001$; male: $p < 0.0001$) (Figure 2A). Regarding differential BALF cell counts, HDM-treated female and male mice had lower mononuclear cell counts than their respective control groups, as determined by Student's t-test (female: $t(3) = 50.669$, $p < 0.001$; male: $t(3) = 5.206$, $p = 0.014$) (Figure 2B). Moreover, the HDM group had higher eosinophil counts (female: $t(4) = -30.613$, $p < 0.001$; male: $t(3) = -4.419$, $p = 0.022$) and neutrophil counts (female: $t(3) = -14.387$, $p < 0.001$; male: $t(3) = -10.634$, $p = 0.002$) than the control group in both female and male mice (Figure 2B).

The Two-Way ANOVA showed a significant effect of HDM treatment on peribronchial inflammation score, with no effect of sex or interaction between factors (treatment: $F(1,26) = 66.093$, $p = <0.01$); sex $F(1,26)$: 0.512, ns; treatment × sex: $F(1,26)$: 0.512, ns), with no effect of sex or interaction between factors. Post hoc analysis revealed that female and male HDM mice had higher score than control groups (female: $p < 0.001$; male: $p < 0.001$). For perivascular inflammation score, the Two-Way ANOVA showed a significant effect of HDM treatment, with no effect of sex or interaction between factors (treatment: $F(1,26) = 205.785$, $p = <0.01$); sex $F(1,26)$: 0.0068, ns; treatment × sex: $F(1,26)$: 0.0068, ns). Post hoc analysis revealed that female and male HDM mice had higher score than control groups (female: $p < 0.001$; male: $p < 0.001$). For PAS score, there was a significant effect of HDM treatment, with no effect of sex or interaction between factors (treatment: $F(1,16) = 338.087$, $p = <0.01$); sex $F(1,16)$: 4.174, ns; treatment × sex: $F(1,16)$: 0.767, ns). Post hoc analysis revealed that female and male HDM mice had higher score than control groups (female: $p < 0.001$; male: $p < 0.001$).

Regarding cytokine concentrations, the Two-Way ANOVA showed no significant effects of HDM treatment, sex, or the interaction between factors on plasma IL-5 levels (treatment: $F(1,28) = 0.7362$, ns; sex: $F(1,28) = 1.0584$, ns; treatment × sex: $F(1,28) = 3.0874$, ns) (Figure 4A). Plasma IL-4 and IL-13 levels

were undetectable. For BALF, the Two-Way ANOVA revealed no significant effects of HDM treatment, sex, or interaction between factors on IL-13 levels (treatment: $F(1,47) = 0.2432$, ns; sex: $F(1,47) = 0.1061$, ns; treatment × sex: $F(1,49) = 1.6035$, ns) (Figure 4B). BALF IL-4 and IL-5 levels were undetectable.

For the lung, the ART ANOVA revealed no significant effects of HDM treatment, sex, or their interaction on IL-4 (treatment: $F(1,42) = 0.1739$, ns; sex: $F(1,42) = 0.7328$, ns; treatment × sex: $F(1,42) = 0.0198$, ns) and IL-13 levels (treatment: $F(1,39) = 2.0602$, ns; sex: $F(1,39) = 0.5769$, ns; treatment × sex: $F(1,39) = 0.7494$, ns) (Figures 4C, E). Although the ART ANOVA revealed main effects of HDM treatment and sex on lung IL-5 levels (treatment: $F(1,39) = 7.8656$, $p = 0.008$; sex: ($F(1,39) = 6.7831$, $p = 0.013$; treatment × sex ($F(1,39) = 0,3173$, ns), Tukey's post hoc comparisons among all groups were not significant after correction for multiple comparisons. However, when the factors were analyzed separately, Student's t-test detected significant differences between the HDM and control groups in females ($t(19) = -2.206$, $p = 0.040$), as well as between female and male mice within the HDM group ($t(31) = -2.763$, $p = 0.010$) (Figure 4D). No significant differences were detected between HDM and control groups in males ($t(20) = 1.533$, $p = 0.141$).

Regarding animals subjected to the plethysmography protocol, statistical analysis of BALF cytokine concentrations showed no significant effects of HDM treatment, sex, or interaction between factors on IL-13 levels (treatment: $F(1,39) = 2.0602$, ns; sex: $F(1,39) = 0.5769$, ns; treatment × sex: $F(1,39) = 0.7494$, ns) (Figure 5A). BALF IL-4 and IL-5 levels were undetectable. In the lung, the ART ANOVA revealed no significant effects of HDM treatment, sex, or interaction between factors on IL-4 (treatment: $F(1,22) = 0$, ns; sex: $F(1,22) = 0.5151$, ns; treatment × sex: $F(1,22) = 0.0035$, ns) and IL-13 levels (treatment: $F(1,18) = 0.8806$, ns; sex: $F(1,18) = 0.0037$, ns; treatment × sex: $F(1,18) = 0.2434$, ns) (Figures 5B, D). Although the ART ANOVA revealed a significant main effect of HDM treatment on lung IL-5 levels (treatment: $F(1,18) = 8.4800$, $p = 0.0093$; sex: $F(1,18) = 2.2367$, ns; treatment × sex: $F(1,18) = 0.0880$, ns), Tukey's post hoc comparisons and subsequent Student's t-test detected no significant pairwise differences between groups (females: $t(9) = -1.909$, $p = 0.089$; males: $t(9) = -1,634$, $p = 0.137$) (Figure 5C).

3.2. Baseline and post-challenge breathing and metabolic patterns in both female and male HDM-treated mice

The Two-Way ANOVA revealed no effect of HDM treatment on V_T, f_R, or V_E in female mice under room air conditions, at either baseline or recovery time points (V_T [treatment: F(1,9) = 0.6971, ns; time: F(1,9) = 0.9302, ns; treatment × time: F(1,9) = 0.1337, ns]; f_R [treatment: F(1,9) = 0.1937, ns; time: F(1,9) = 1.2377, ns; treatment × time: F(1,9) = 0.0072, ns]; V_E [treatment: F(1,9) = 0.1090, ns; time: F(1,9) = 0.1954, ns; treatment × time: F(1,9) = 0.0156, ns]) (Figure 6A, B, C). Similarly, the Two-Way ANOVA revealed no effect of HDM treatment on V_T in male mice; however, it revealed a significant effect of time (treatment: F(1,9) = 0.9591, ns; time: F(1,9) = 7.8562, p = 0.0206; treatment × time: F(1,9) = 3.7512, ns). Post hoc analysis indicated that V_T in control males was higher during recovery compared with baseline (p = 0.01) (Figure 7A). For f_R, the Two-Way ANOVA revealed an interaction between factors in male mice (treatment: F(1,9) = 0.9591, ns; time: F(1,9) = 2.3790, ns; treatment × time: F(1,9) = 13.7085, p = 0.0049). Post hoc analysis showed that f_R was lower during recovery compared with baseline in control males, and that the HDM group exhibited higher f_R compared with the control group during the same time point (p = 0.02) (Figure 7B).

With regard to T_{insp}, the Two-Way ANOVA revealed no effects of HDM treatment, time, or interaction between factors in female mice under room air conditions (treatment: F(1,9) = 3.3503, ns; time: F(1,9) = 0.0510, ns; treatment × time: F(1,9) = 1.3856, ns) (Figure 6D); however, it revealed a significant effect of HDM treatment on T_{insp} in male mice, with no effect of time or interaction between factors (treatment: F(1,9) = 13.1429, p = 0.0055; time: F(1,9) = 0.00001, ns; treatment × time: F(1,9) = 2.2198, ns). The post hoc analysis indicated that T_{insp} was lower in HDM male mice compared to the control group during recovery (p = 0.001) (Figure 7D).

For T_{exp}, HDM treatment or time did not induce significant changes in female mice at either baseline or recovery (treatment: F(1,9) = 0.0812, ns; time: F(1,9) = 1.0828, ns; treatment × time: F(1,9) = 0.4297, ns) (Figure 6E). By contrast, the Two-Way ANOVA revealed an interaction between factors on T_{exp} in male mice under room air conditions (treatment: F(1,9) = 0.9474, ns; time: F(1,9)

= 4.5246, ns; treatment × time: F(1,9) = 16.5358, p = 0.0028). Post hoc analysis indicated that T_{exp} in control males was higher during recovery compared with baseline (p = 0.0023) (Figure 7E).

Concerning cycle duration, there were no significant effects of HDM treatment, time, or interaction between factors in female mice under room air conditions (treatment: F(1,9) = 0.1315, ns; time: F(1,9) = 1.1724, ns; treatment × time: F(1,9) = 0.0851, ns) (Figure 6F). However, the Two-Way ANOVA revealed an interaction between factors on cycle duration in male mice under the same air condition (treatment: F(1,9) = 2.5397, ns; time: F(1,9) = 2.9105, ns; treatment × time: F(1,9) = 18.8281, p = 0.0018). Post hoc analysis indicated that cycle duration was higher in control males during recovery than at baseline (p = 0.0027) and in the HDM group (p = 0.0194) (Figure 7F).

In terms of metabolic parameters, the Two-Way ANOVA revealed a significant effect of HDM treatment on VO_2 in female mice under room air conditions, with no effect of time or interaction between factors (treatment: F(1,9) = 6.4451, p = 0.0317; time: F(1,9) = 0.7605, ns; treatment × time: F(1,9) = 0.2299, ns). Post hoc analysis indicated that VO_2 was lower in HDM female mice during baseline compared to the control group (p = 0.0338) (Figure 6G). In male mice, there were no significant effects of HDM treatment, time, or interaction between factors on VO_2 (treatment: F(1,9) = 1.1892, ns; time: F(1,9) = 0.3152, ns; treatment × time: F(1,9) = 2.1139, ns) (Figure 7G).

Regarding VCO_2, post hoc analysis showed that it was higher in control females at baseline than in both recovery (p = 0.0415) and the HDM group (p = 0.0223) (Figure 6H). However, the Two-Way ANOVA detected no significant effects of HDM exposure, time, or their interaction (treatment: F(1,9) = 4.2600, ns; time: F(1,9) = 3.4523, ns; treatment × time: F(1,9) = 2.722, ns). In males, post hoc analysis showed that VCO_2 was lower during recovery than at baseline in the HDM group (p = 0.0357) (Figure 7H). The Two-Way ANOVA likewise detected no significant effects of HDM exposure, time, or their interaction (treatment: F(1,9) = 0.0060, ns; time: F(1,9) = 2.1415, ns; treatment × time: F(1,9) = 3.4743, ns).

For RQ, there were no significant effects of HDM treatment, time, or interaction between factors in female (treatment: F(1,9) = 0.34848, ns; time:

F(1,9) = 0.3694, ns; treatment × time: F(1,9) = 3.3207, ns) and male mice (treatment: F(1,9) = 1.6826, ns; time: F(1,9) = 0.1779, ns; treatment × time: F(1,9) = 0.0089, ns) (Figures 6I, 7I).

In both female and male mice, the Two-Way ANOVA revealed no effects of HDM treatment, time, or interaction between factors on V_E/VO_2 (female [treatment: F(1,9) = 3.7898, ns; time: F(1,9) = 0.3204, ns; treatment × time: F(1,9) = 0.0552, ns]; male [treatment: F(1,9) = 1.6212, ns; time: F(1,9) = 0.3306, ns; treatment × time: F(1,9) = 0.3198, ns]) (Figures 6J, 7J).

For V_E/VCO_2, there were no significant effects of HDM treatment, time, or interaction between factors in female mice (treatment: F(1,9) = 1.4724, ns; time: F(1,9) = 0.7595, ns; treatment × time: F(1,9) = 0.4145, ns) (Figure 6K). In males, post hoc analysis showed that V_E/VCO_2 was higher during recovery compared with baseline in the HDM group (p = 0.0338), although no significant effects of HDM exposure, time, or their interaction were detected by the Two-Way ANOVA (treatment: F(1,9) = 0.3127, ns; time: F(1,9) = 3.5908, ns; treatment × time: F(1,9) = 2.1798, ns) (Figure 7K).

Finally, there was a significant effect of time on T_B in both female and male mice, with no effect of HDM treatment or interaction between factors (female [treatment: F(1,9) = 0.1228, ns; time: F(1,9) = 14.1130, p = 0.0045; treatment × time: F(1,9) = 0.2181, ns]; male [treatment: F(1,9) = 0.0028, ns; time: F(1,9) = 12.2146, p = 0.0067; treatment × time: F(1,9) = 0.0037, ns]). Post hoc analysis showed that T_B was lower during recovery compared with baseline in both control and HDM-treated mice (control female: p = 0.0187; HDM female: p = 0.0373; control male: p = 0.0394; HDM male: p = 0.0313) (Figures 6L, 7L).

3.3. Ventilatory and metabolic responses to hypoxia in both female and male HDM-treated mice

During hypoxic challenge, no effect of HDM treatment or time was observed on V_T in female mice (treatment: F(1,9) = 0.0048, ns; time: F(1,9) = 1.1015, ns; treatment × time: F(1,9) = 0.0012, ns) (Figure 8A). In males, the Two-Way ANOVA revealed a significant effect of time on V_T, with no effect of HDM treatment or interaction between factors (treatment: F(1,9) = 0.8877, ns; time:

$F(1,9) = 6.8554$, $p = 0.0278$; treatment × time: $F(1,9) = 0.2366$, ns); however, post hoc analysis showed no significant differences between groups (Figure 9A).

With regard to f_R, although the Two-Way ANOVA revealed no significant effects of HDM treatment, time, or their interaction (treatment: $F(1,9) = 2.2480$, ns; time: $F(1,9) = 2.4475$, ns; treatment × time: $F(1,9) = 3.4947$, ns), post hoc analysis showed a reduction in f_R after 20 min compared to 10 min of hypoxia in HDM female mice ($p = 0.0313$) (Figure 8B). In males, the Two-Way ANOVA revealed significant effects of HDM treatment and time on f_R, with no interaction between them (treatment: $F(1,9) = 8.2104$, $p = 0.0186$; time: $F(1,9) = 16.0201$, $p = 0.0030$; treatment × time: $F(1,9) = 0.9412$, $p = 0.3572$). Post hoc analysis showed that f_R was higher in HDM-treated males compared with controls at both 10 and 20 min of hypoxia exposure (10 min: $p = 0.0356$; 20 min: $p = 0.0119$) (Figure 9B). In addition, post hoc analysis also showed a reduction in f_R after 20 min compared with 10 min of hypoxia in control males ($p = 0.0083$) (Figure 9B).

For V_E, no effect of HDM exposure or time was detected by the Two-Way ANOVA in female mice during hypoxia (treatment: $F(1,9) = 1.9048$, ns; time: $F(1,9) = 0.0612$, ns; treatment × time: $F(1,9) = 1.4259$, ns) (Figure 8C). In contrast, the Two-Way ANOVA revealed a significant effect of HDM treatment on V_E in male mice, with no effect of time or interaction between factors (treatment: $F(1,9) = 17.3502$, $p = 0.0024$; time: $F(1,9) = 0.2091$, ns; treatment × time: $F(1,9) = 0.5035$, ns). Post hoc analysis showed that V_E was higher in HDM-treated males compared with controls at both 10 and 20 min of hypoxia exposure (10 min: $p = 0.0331$; 20 min: $p = 0.0066$) (Figure 9C).

Although the Two-Way ANOVA revealed no significant effects of HDM treatment, time or interaction between factors on T_{insp} in female mice during hypoxia (treatment: $F(1,9) = 0.1130$, ns; time: $F(1,9) = 0.1246$, ns; treatment × time: $F(1,9) = 0.8814$, ns), post hoc analysis showed that T_{insp} was lower in HDM-treated females compared with controls after 10 min of gas exposure ($p = 0.0363$) (Figure 8D). In males, there were significant effects of HDM treatment and time on T_{insp} (treatment: $F(1,9) = 6.3012$, $p = 0.0332$; time: $F(1,9) = 16.4610$, $p = 0.0028$; treatment × time: $F(1,9) = 3.0525$, ns). Post hoc analysis showed that T_{insp} was lower in HDM-treated males compared with controls at both 10 and 20 min of hypoxia exposure (10 min: $p = 0.0190$; 20 min: $p = 0.0461$) (Figure 9D).

Moreover, post hoc analysis also showed an increase in T_{insp} after 20 min of the respiratory challenge compared with 10 min in control males ($p = 0.0034$) (Figure 9D).

In relation to T_{exp}, no significant effects of HDM treatment, time, or interactions between them were detected by the Two-Way ANOVA in female mice during hypoxia (treatment: $F(1,9) = 3.8565$, ns; time: $F(1,9) = 1.7671$, ns; treatment × time: $F(1,9) = 0.0259$, ns) (Figure 8E). However, the Two-Way ANOVA revealed a significant effect of HDM treatment on T_{exp} in male mice exposed to hypoxia, with no effect of time or interaction between factors (treatment: $F(1,9) = 5.5557$, $p = 0.0428$; time: $F(1,9) = 0.0949$, ns; treatment × time: $F(1,9) = 0.0435$, ns). Post hoc analysis showed that T_{exp} was lower in HDM-treated males compared with controls after 20 min of hypoxia exposure ($p = 0.0481$) (Figure 9E).

Similarly to T_{exp}, the Two-Way ANOVA revealed no effects of HDM treatment, time, or interactions between factors on cycle duration in female mice exposed to hypoxia (treatment: $F(1,9) = 0.7255$, ns; time: $F(1,9) = 0.7240$, ns; treatment × time: $F(1,9) = 3.6065$, ns) (Figure 8F). In contrast, the Two-Way ANOVA revealed significant effects of HDM treatment, time, and their interaction in male mice (treatment: $F(1,9) = 8.4728$, $p = 0.0172$; time: $F(1,9) = 20.5957$, $p = 0.0014$, treatment × time: $F(1,9) = 6.1503$, $p = 0.0349$). Post hoc analysis showed that cycle duration was lower in HDM-treated males compared with controls at both 10 and 20 min of hypoxia exposure (10 min: $p = 0.0461$; 20 min: $p = 0.0089$) (Figure 9F). Moreover, post hoc analysis also showed an increase in cycle duration after 20 min compared with 10 min of hypoxia in control males ($p = 0.0010$) (Figure9).

Because significant baseline differences between HDM and control female mice were observed for VO_2 and VCO_2, the hypoxic responses of VO_2, VCO_2, RQ, V_E/VO_2, V_E/VCO_2 are presented as delta values in females. For ΔVO_2, there was a significant effect of time in female mice exposed to hypoxia (treatment: $F(1,9) = 1.4093$, ns; time: $F(1,9) = 21.5526$, $p = 0.0012$, treatment × time: $F(1,9) = 3.0461$, ns). Post hoc analysis showed an increase in ΔVO_2 after 20 min compared with 10 min of hypoxia exposure in HDM-treated female mice ($p = 0.001$), and higher ΔVO_2 in the HDM group compared with the control group after

20 min of hypoxia exposure ($p = 0.04$) (Figure 8G). In males, the Two-Way ANOVA detected an effect of time on VO_2 under hypoxic conditions, with no effect of HDM treatment or interaction between factors (treatment: $F(1,9) = 0.7895$, ns; time: $F(1,9) = 8.8500$, $p = 0.0155$, treatment × time: $F(1,9) = 0.0275$, ns). Post hoc analysis showed an increase in VO_2 after 20 min compared with 10 min of hypoxia exposure in HDM-treated male mice ($p = 0.0447$) (Figure 9G).

The Two-Way ANOVA revealed significant effects of HDM exposure and time on ΔVCO_2 in female mice exposed to hypoxia, with no interaction between factors (treatment: $F(1,9) = 5.8755$, $p = 0.0415$; time: $F(1,9) = 13.9674$, $p = 0.0057$, treatment × time: $F(1,9) = 0.0623$, ns). Post hoc analysis showed a reduction in ΔVCO_2 after 20 min compared with 10 min of hypoxia exposure in control female mice ($p = 0.0315$), and lower ΔVCO_2 in the HDM group compared with the control group after 20 min of hypoxia exposure ($p = 0.0261$) (Figure 8H). In males, there was also a significant effect of time on VCO_2 during hypoxia exposure, with no effect of HDM treatment or interaction between factors (treatment: $F(1,9) = 0.0188$, ns; time: $F(1,9) = 69.3211$, $p = 0.00001$, treatment × time: $F(1,9) = 0.3296$, ns). Post hoc analysis showed a reduction in VCO_2 after 20 min compared with 10 min of hypoxia exposure in both control and HDM groups (control: $p = 0.0005$; HDM: $p = 0.00009$) (Figure 9H).

Regarding ΔRQ, there was a significant effect of time in females under hypoxic conditions, with no effect of HDM treatment or interaction between factors (treatment: $F(1,9) = 0.3906$, ns; time: $F(1,9) = 27.4416$, $p = 0.0007$, treatment × time: $F(1,9) = 1.9471$, ns). Post hoc analysis showed a reduction in ΔRQ after 20 min compared with 10 min of hypoxia exposure in both control and HDM groups (control: $p = 0.0263$; HDM: $p = 0.0015$) (Figure 8I). In males, the Two-Way ANOVA also revealed an effect of time during hypoxia, with no effect of HDM treatment or interaction between factors (treatment: $F(1,9) = 0.7565$, ns; time: $F(1,9) = 12.4812$, $p = 0.0063$, treatment × time: $F(1,9) = 0.6173$, ns). Post hoc analysis showed a reduction in RQ after 20 min compared with 10 min of hypoxia exposure in the HDM group ($p = 0.010$) (Figure 9I).

In female mice, the Two-Way ANOVA revealed an effect of time on $\Delta V_E/VO_2$ during hypoxia, with no effect of HDM treatment or interaction between factors (treatment: $F(1,9) = 0.2106$, ns; time: $F(1,9) = 11.1256$, $p = 0.0087$,

treatment × time: F(1,9) = 4.1602, ns). Post hoc analysis showed a decrease in $\Delta V_E/VO_2$ after 20 min compared with 10 min of hypoxia exposure in HDM-treated females (p = 0.0031) (Figure 8J). In males, no significant effects of HDM treatment, time, or interaction between factors were observed on V_E/VO_2 under hypoxic conditions (treatment: F(1,9) = 4.0278, ns; time: F(1,9) = 3.3877, ns; treatment × time: F(1,9) = 0.3099, ns) (Figure 9J).

Concerning $\Delta V_E/VCO_2$, although the Two-Way ANOVA revealed a significant effect of time in female mice exposed to hypoxia (treatment: F(1,9) = 0.1917, ns; time: F(1,9) = 8.0135, p = 0.0221; treatment × time: F(1,9) = 0.0337, ns), post hoc analysis showed no significant differences between groups (control: p = 0.0656; HDM: p = 0.0981) (Figure 8K). In contrast, the Two-Way ANOVA revealed a significant effect of time on V_E/VCO_2 in males during hypoxia, with no effect of HDM treatment or interaction between factors (treatment: F(1,9) = 2.9861, ns; time: F(1,9) = 11.5787, p = 0.0078; treatment × time: F(1,9) = 1.5988, ns). Post hoc analysis showed that V_E/VCO_2 was higher after 20 min compared with 10 min of hypoxia exposure in HDM-treated males (p = 0.007) (Figure 9K).

Finally, there was a significant effect of time on T_B in female mice exposed to hypoxia, with no effect of HDM treatment or interaction between factors (treatment: F(1,9) = 0.4765, ns; time: F(1,9) = 58.1629, p = 0.00003; treatment × time: F(1,9) = 0.0109, ns). Post hoc analysis showed that T_B was lower after 20 min compared with 10 min of hypoxia exposure in both the control and HDM groups (control: p = 0.0005; HDM: p = 0.0003) (Figure 8L). In males, the Two-Way ANOVA also revealed a significant effect of time on T_B under hypoxic conditions, with no effect of HDM treatment or interaction between factors (treatment: F(1,9) = 0.8094, ns; time: F(1,9) = 13.4873, p = 0.0051; treatment × time: F(1,9) = 2.7045, ns). However, post hoc analysis showed that T_B was lower after 20 min compared with 10 min of hypoxia exposure only in control males (p = 0.0057) (Figure 9L).

3.4. Ventilatory and metabolic responses to hypercapnia in both female and male HDM-treated mice

The Two-Way ANOVA revealed no significant effects of HDM treatment, time, or interaction between factors on V_T in both female and male mice under

hypercapnic conditions (female [treatment: F(1,9) = 1.2643, ns; time: F(1,9) = 0.1124, ns; treatment × time: F(1,9) = 0.2419, ns]; male [treatment: F(1,9) = 1.6562, ns; time: F(1,9) = 0,0364; treatment × time: F(1,9) = 0,2451, ns]) (Figures 10A, 11A). In the same way, no effects of HDM treatment, time, or interaction between them were observed on V_E in both female and male mice exposed to hypercapnia (female [treatment: F(1,9) = 0.4073, ns; time: F(1,9) = 0.0015, ns; treatment × time: F(1,9) = 0.6777, ns]; male [treatment: F(1,9) = 0.3551, ns; time: F(1,9) = 0.0361; treatment × time: F(1,9) = 1.1035, ns]) (Figures 10C, 11C).

Regarding f_R, the Two-Way ANOVA revealed a significant effect of HDM treatment in female mice exposed to hypercapnia, with no effects of time or interaction between factors (treatment: F(1,9) = 23.9543, p = 0.0008; time: F(1,9) = 0.2366, ns; treatment × time: F(1,9) = 0.3185, ns). Post hoc analysis showed that f_R was higher in HDM-treated females compared to controls after 10 and 20 min of hypercapnia exposure (10 min: p = 0.0001; 20 min: p = 0,0062) (Figure 10B). In males, the Two-Way ANOVA revealed significant effects of HDM treatment and interaction between factors on f_R under hypercapnia conditions (treatment: F(1,9) = 20.7340, p = 0.0013; time: F(1,9) = 0.2485, ns; treatment × time: F(1,9) = 16.1658, p = 0.0030). Post hoc analysis showed that f_R was higher in the HDM-treated males compared with controls at both 10 and 20 min of hypercapnia (10 min: p = 0.0356; 20 min: p = 0.0119) (Figure 11B). Moreover, post hoc analysis also showed an increase in f_R after 20 min compared with 10 min of hypercapnia in control males (p = 0.0409), whereas a decrease was observed in the HDM group (p = 0.0085) (Figure 11B).

For T_{insp}, there were no effects of HDM treatment, time, or interaction between factors in female mice during the hypercapnic challenge (treatment: F(1,9) = 2.7471, ns; time: F(1,9) = 1.6663, ns; treatment × time: F(1,9) = 1.4908, ns) (Figure 10D). By contrast, the Two-Way ANOVA revealed significant effect of HDM treatment and interaction between factors on T_{insp} in male mice exposed to hypercapnia (treatment: F(1,9) = 24.6126, p = 0.0007, time: F(1,9) = 2.9213, ns; treatment × time: F(1,9) = 9.3375, p = 0.0136). Post hoc analysis showed that T_{insp} was lower in the HDM-treated males compared with controls at both 10 and 20 min of hypercapnia (10 min: p = 0.0006; 20 min: p = 0.0014) (Figure 11D).

Additionally, post hoc analysis also showed a reduction in T_{insp} after 20 min compared with 10 min of hypercapnia in control males ($p = 0.0103$) (Figure 11D).

Regarding T_{exp}, the Two-Way ANOVA revealed a significant effect of HDM treatment in females under hypercapnic conditions, with no effect of time or interaction between factors (treatment: $F(1,9) = 18.5698$, $p = 0.0019$; time: $F(1,9) = 0.0074$, ns; treatment × time: $F(1,9) = 0.0582$, ns). Post hoc analysis showed that T_{exp} was lower in HDM-treated females than in controls at both 10 and 20 min of hypercapnia (10 min: $p = 0.0017$; 20 min: $p = 0.0110$) (Figure 10E). In males, there were no effects of HDM treatment or time, but there was a significant interaction between factors on T_{exp} during hypercapnia (treatment: $F(1,9) = 0.0086$, ns; time: $F(1,9) = 1.6851$, ns; treatment × time: $F(1,9) = 7.8819$, $p = 0.0204$). Post hoc analysis showed an increase in T_{exp} after 20 min compared with 10 min of hypercapnia in HDM-treated males ($p = 0.0139$) (Figure 11E).

In female mice, there was a significant effect of HDM treatment on CD during the hypercapnic challenge, with no effect of time or interaction between factors (treatment: $F(1,9) = 6.1796$, $p = 0.0346$; time: $F(1,9) = 0.2235$, ns; treatment × time: $F(1,9) = 0.0531$, ns). Post hoc analysis showed that CD was lower in the HDM-treated females compared with controls at both 10 and 20 min of hypercapnia (10 min: $p = 0.0306$; 20 min: $p = 0.0416$) (Figure 10F). For males, the Two-Way ANOVA revealed a significant effect of HDM treatment and interaction between factors on CD under hypercapnic conditions (treatment: $F(1,9) = 24.6266$, $p = 0.0007$; time: $F(1,9) = 0.1401$, ns; treatment × time: $F(1,9) = 19.4735$, $p = 0.0016$). Post hoc analysis showed that CD was lower in HDM-treated males compared with controls after both 10 and 20 min of hypercapnia exposure (10 min: $p = 0.0003$; 20 min: $p = 0.0025$) (Figure 11F). In addition, post hoc analysis also revealed a decrease in CD after 20 min compared with 10 min of hypercapnia in control males ($p = 0.0101$), whereas an increase was observed in the HDM group ($p = 0.0150$) (Figure 11F).

Because significant baseline differences between HDM and control female mice were observed for VO_2 and VCO_2, the hypercapnic responses of VO_2, VCO_2, RQ, V_E/VO_2, and V_E/VCO_2 are presented as delta values in females. For ΔVO_2, the post hoc analysis showed a significant effect of HDM treatment in female mice exposed to hypercapnia ($p = 0.0365$), despite the Two-Way ANOVA

revealing no effects of HDM treatment, time, or interaction between factors (treatment: $F(1,9) = 4.0536$, $p = 0.0749$); time: $F(1,9) = 0.4397$, ns, treatment × time: $F(1,9) = 0.3766$, ns) (Figure 10G). In contrast, the Two-Way ANOVA revealed an effect of HDM treatment on VO_2 in male mice during hypercapnia, with no effect of time or interaction between factors (treatment: $F(1,9) = 6.2305$, $p = 0.0340$; time: $F(1,9) = 0.0139$, ns, treatment × time: $F(1,9) = 1.3438$, ns). Post hoc analysis showed that VO_2 was higher in HDM-treated males compared with controls after 10 min of hypercapnia exposure ($p = 0.0217$) (Figure 11G).

In regard to ΔVCO_2, the Two-Way ANOVA revealed a significant effect of time and an interaction between factors in female mice under hypercapnic conditions, with no isolated effect of HDM treatment (treatment: $F(1,4) = 0.0008$, ns; time: $F(1,4) = 35.2728$, $p = 0.0040$; treatment × time: $F(1,4) = 10.6669$, $p = 0.0309$). Post hoc analysis showed an increase in ΔVCO_2 after 20 min compared with 10 min of hypercapnic exposure in HDM-treated females ($p = 0.0048$) (Figure 10H). In males, there was also a significant effect of time on VCO_2 during hypercapnia, with no effect of HDM treatment or interaction between factors (treatment: $F(1,9) = 0.92098$, ns; time: $F(1,9) = 8.1151$, $p = 0.0230$, treatment × time: $F(1,9) = 0,0101$, ns). Post hoc analysis showed an increase in VCO_2 after 20 min compared with 10 min of hypercapnia exposure in both control and HDM groups (control: $p = 0.0190$; HDM: $p = 0.0097$) (Figure 11H).

There was an effect of time and an interaction between factors on ΔRQ in females during hypercapnic challenge, with no isolated effect of HDM treatment (treatment: $F(1,9) = 7.7050$, $p = 0.0500$; time: $F(1,9) = 82.4773$, $p = 0.\ 00008$, treatment × time: $F(1,9) = 9.0278$, $p = 0.0397$). Post hoc analysis showed an increase in ΔRQ after 20 min compared with 10 min of hypercapnic exposure in both control and HDM groups (control: $p = 0.0062$; HDM: $p = 0.0017$), and a lower ΔRQ in HDM-female mice compared with control after 10 min of hypercapnia ($p = 0.0113$) (Figure 10I). In males, the Two-Way ANOVA also revealed an effect of time under hypercapnic conditions, with no effect of HDM treatment or interaction between factors (treatment: $F(1,9) = 1.2474$, ns; time: $F(1,9) = 11.0487$, $p = 0.0111$; treatment × time: $F(1,9) = 0.000001$, ns). Post hoc analysis showed an increase in RQ at 20 min compared with 10 min of hypercapnic exposure in the HDM group ($p = 0.0449$) (Figure 11I).

There were no significant effects of HDM treatment, time, or the interaction between factors on $\Delta V_E/VO_2$ in female mice exposed to hypercapnia (treatment: $F(1,9) = 2.1305$, ns; time: $F(1,9) = 0.4770$, ns; treatment × time: $F(1,9) = 0.0530$, ns). (Figure 10J). In males, the Two-Way ANOVA revealed a significant effect of HDM on V_E/VO_2 under hypercapnic conditions (treatment: $F(1,9) = 5.5015$, $p = 0.0436$; time: $F(1,9) = 0.3462$, ns; treatment × time: $F(1,9) = 1.4821$, ns). Post hoc analysis showed that V_E/VO_2 was lower in HDM-treated males compared with the control group after 10 min of hypercapnic exposure ($p = 0.0263$) (Figure 11J).

Concerning $\Delta V_E/VCO_2$, a mixed-effects model on ranks revealed a significant effect of time in female mice during hypercapnic challenge (treatment: $F(1,9.15) = 1.3130$, ns; $F(1,4.95) = 20.09$, $p = 0.0067$); treatment × time: $F(1,4.95) = 3.5190$, ns). Post hoc analysis showed a decrease in $\Delta V_E/VCO_2$ after 20 min compared with 10 min of hypercapnic exposure in HDM-exposed females ($p = 0,0110$) (Figure 10K). In males, although the Two-Way ANOVA revealed an effect of time on V_E/VCO_2 during hypercapnia, with no effect of HDM treatment or interaction between factors (treatment: $F(1,9) = 0.1054$, ns; time: $F(1,9) = 8.1151$, $p = 0.0230$; treatment × time: $F(1,9) = 0.0101$, ns), post hoc analysis showed no significant differences between groups (control: $p = 0.0761$; HDM: $p = 0.0867$) (Figure 11K).

Although the Two-Way ANOVA revealed an effect of time on T_B in female mice exposed to hypercapnia, with no effect of HDM treatment or interaction between factors (treatment: $F(1,9) = 0.1172$, ns; time: $F(1,9) = 5.3463$, $p = 0.0460$; treatment × time: $F(1,9) = 0.00002$, ns), post hoc analysis showed no significant differences between groups (control: $p = 0.1527$; HDM: $p = 0.1198$) (Figure 10L). In males, the Two-Way ANOVA revealed significant effects of HDM exposure and time on T_B under hypercapnic conditions (treatment: $F(1,9) = 5.1737$, $p = 0.0489$; time: $F(1,9) = 10.9138$, $p = 0.0091$; treatment × time: $F(1,9) = 0.0155$, ns). Post hoc analysis showed that T_B was higher in HDM-treated males than in controls after 20 min of hypercapnic exposure ($p = 0.0425$), but lower than at 10 min of hypercapnia in the same group ($p = 0.0315$) (Figure 11L).

4. DISCUSSION

4.1. HDM-induced asthma phenotype and sex differences

Combined histological analysis and total and differential cell counts in the bronchoalveolar lavage fluid (BALF) demonstrated that house dust mite (HDM) exposure induced robust eosinophilic airway inflammation in female and male mice, consistent with a classical allergic asthma phenotype (Akar-Ghibril et al., 2020). This inflammatory profile was characterized by marked eosinophil infiltration in the airways, enhanced peribronchial and perivascular inflammatory cuffs, and mucus accumulation, as evidenced by increased PAS-positive staining. Together, these findings align with the well-established type 2 (Th2)-driven airway inflammatory response in experimental asthma models (Aun et al., 2017; Carroll et al., 2023; Fallon and Schwartz, 2020).

Although BALb/c mice are most often used because of their propensity for a Th2 immunological response, which allows these models to better reproduce key features of allergic asthma, including airway inflammation, remodeling, and hyperresponsiveness (Boucher et al., 2021), increasing evidence indicates that C57BL/6 mice also develop robust allergic airway inflammation following exposure to HDM (Allgire et al., 2023; Makino et al., 2021; Raemdonck et al., 2016) In the present study, HDM-challenged C57BL/6 mice exhibited marked inflammatory alterations, as demonstrated by increased eosinophils in the BALF, peribronchial and perivascular inflammatory infiltrates, and mucus production. These findings reinforce the suitability of the C57BL/6 strain for experimental models of HDM-induced allergic asthma. Nevertheless, an important limitation of this study is the absence of an assessment of airway responsiveness, which is strongly recommended for more comprehensive validation of murine asthma models (Finkelman, 2008).

Regarding sex differences in asthma prevalence and severity, it is well documented that boys have an increased prevalence of asthma during childhood, whereas women become more affected than men as adults (Chowdhury et al., 2021). These findings suggest that sexual hormones play an important role in asthma pathogenesis, as demonstrated by several studies showing that estrogen may enhance inflammatory responses, whereas testosterone and other androgens appear to exert anti-inflammatory effects (Ambhore et al., 2019; Becerra-Diaz et al., 2018; Blanquart et al., 2022; Stölting et al., 2026). In that

regard, a recent study evaluated sex differences in the HDM-induced asthma model in C57BL/6 mice, demonstrating sex-dependent inflammatory responses (Mostafa et al., 2022). Interestingly, no sex differences were detected in total BALF cell counts, although males exhibited higher eosinophil counts in the differential cell analysis. Similarly, in the present study, total BALF cell counts were not influenced by sex, and the lack of sex-related differences in the differential cell counts may be attributable to the reduced sample size (n = 3 for females and n = 2 for males).

When accounting for the cytokine profile, the authors demonstrated higher lung and BALF levels of IL-33, IL-1β, and IL-21 in females, whereas IL-9 levels were increased in the lung tissue of males (Mostafa et al., 2022). In contrast, no sex differences in IL-5 levels were observed in HDM-challenged mice, although naïve females exhibited higher IL-5 levels in both BALF and lung tissue compared with males (Mostafa et al., 2022). Conversely, in the present study, female HDM-treated mice showed higher lung IL-5 levels than males, while no sex-related differences were detected in control animals.

An important caveat of both the present study and the study by Mostafa and colleagues (2022) is the use of post-pubertal mice. As discussed above, sex bias in asthma manifestation is age-dependent, with women exhibiting more severe symptoms than men after puberty. Thus, the results reported in both studies are most likely representative of sex-related differences in adulthood, when estradiol has been associated with pro-inflammatory responses in asthma. However, the pro-inflammatory role of estrogen may not be absolute, as differential expression of estrogen receptors also influences airway hyperreactivity and remodeling. In this context, estrogen signaling through estrogen receptor β (ERβ) has been associated with reduced airway hyperresponsiveness and decreased eosinophil infiltration (Ambhore et al., 2019; Fuseini et al., 2017; Yung et al., 2018). Therefore, the role of sex steroids in HDM-induced airway inflammation requires further investigation.

Another important point of the present study is the absence of significant changes in lung and BALF IL-4 and IL-13 levels of HDM-challenged mice, which does not necessarily exclude the establishment of a Th2-like inflammatory response. In that regard, previous studies have demonstrated that C57BL/6 mice

develop less robust IL-4 and IL-13 responses than BALb/c mice following HDM exposure, although both strains exhibit lung inflammation and mucus production consistent with a predominant Th2-type response (Doherty et al., 2012; Gold et al., 2014; Sahu et al., 2010; Yasuda et al., 2020). Moreover, the detection of these cytokines may be highly dependent on the timing of sample collection. In fact, experimental evidence has shown that IL-4 and IL-13 concentrations rise rapidly after the final allergen exposure, peaking within 2–4 h and declining markedly within 24 h (Gregory et al., 2009). In the present study, tissue collection was performed 3 days after the final challenge, which may have contributed to the lack of detectable changes in these cytokines despite alterations consistent with allergic airway inflammation.

Finally, we cannot rule out the possibility of a mixed Th1/Th2-skewed response following an HDM challenge. The study by Mostafa and colleagues (2022) demonstrated that, unlike BALb/c mice, HDM-driven changes in the lung cytokine profile of female C57Bl/6 mice are characterized predominantly by a Th1-skewed response, with high levels of macrophage inflammatory protein-2 (MIP-2), interferon gamma-induced protein 10 (IP-10), and IL-1β (Hammad and Lambrecht, 2021). However, cytokines associated with Th2-type responses, such as IL-33 and IL-21, were also elevated in female C57BL/6 mice following HDM exposure. These findings suggest that female C57BL/6 mice may develop a mixed Th1/Th2-skewed response after HDM challenge, depending on the dose and duration of allergen exposure. Overall, our data indicate that HDM-challenged mice developed a predominantly Th2-biased inflammatory response, characterized by eosinophilia and elevated lung IL-5 levels.

4.2. HDM-induced airway inflammation alters baseline and post-challenge breathing and metabolic patterns in a sex-dependent manner

Although HDM-exposed mice presented a marked airway inflammation, no basal ventilatory parameters were affected in both female and male mice. Similarly, OVA sensitization and challenge did not alter these parameters in male Brown Norway rats under normoxic and normocapnic conditions (Morgan et al., 2024). In contrast to our study and that of Morgan et al. (2024), a recent study using double-chamber plethysmography reported reduced tidal volume (V_T) and a trend toward decreased minute ventilation (V_E) ($p = 0.05$) in female C57BL/6

mice exposed to HDM under room air conditions. Thus, similar V_T values between control and HDM or OVA groups may suggest that there was no mechanical impairment of airway inflammation induced by allergen exposure. Indeed, pulmonary function testing with the FlexiVent system in OVA-exposed rats showed no treatment effect on the parameters assessed. Moreover, the lack of compensatory changes in basal respiratory frequency (f_R) in HDM-exposed mice may further support this interpretation; however, this remains speculative, as definitive conclusions require appropriate measurements.

During recovery, only male mice presented changes in ventilatory parameters after the respiratory challenge. Specifically, control males presented increased V_T and decreased f_R compared with baseline. This pattern was further supported by increased expiration time (T_{exp}) and cycle duration. In HDM-exposed males, there were no changes in V_T or f_R compared with baseline; however, they exhibited a faster breathing pattern than controls, characterized by higher f_R and shorter inspiration time (T_{insp}) and cycle duration. These findings reflect a shift in the post-challenge response pattern following allergen exposure, in which control males primarily increased V_T, whereas HDM-exposed males relied more on an increased f_R. From a functional perspective, this may represent a more efficient ventilatory strategy in control mice following a respiratory challenge, as increased V_T allows a greater volume of air to reach the lungs under resting conditions (Reid et al., 2023).

Regarding baseline metabolic parameters, only female mice exhibited impairments in allergen exposure, characterized by decreased oxygen consumption (VO_2) and CO_2 production (VCO_2). This pattern may reflect lower aerobic metabolism following HDM-induced airway inflammation, particularly in females. Indeed, there are several pieces of evidence of metabolic dysfunction in asthma that are associated with the obese asthma phenotype, including metabolic reprogramming, increased oxygen reactive species, decreased ATP production, increased lipidic metabolism and glycolysis, and lower aerobic capacity during exercise (Cortés-Télles et al., 2015; Hartsoe et al., 2024; Peters et al., 2018). Thus, our findings suggest that allergen-induced airway inflammation altered metabolic regulation in females, supporting this model as a useful tool to investigate the pathways through which asthma contributes to

metabolic dysfunction. This is particularly relevant in women, given that adult-onset obese asthma is more prevalent in females (Peters et al., 2018).

Allergen exposure combined with the chemosensory stimulus in males led to decreased VCO_2 and increased respiratory equivalent for CO_2 (V_E/VCO_2) during recovery compared with baseline, suggesting a potential reduction in metabolic rate, although no significant changes were observed in VO_2. Moreover, the increase in V_E/VCO_2 under these conditions indicates that a greater ventilatory effort was required to eliminate a relatively lower amount of CO_2 produced, suggesting that the effect of the respiratory challenge may have been more pronounced in HDM-exposed males, even though no significant differences were observed within the control group. The mechanisms underlying the effects of airway inflammation on respiratory control centers will be discussed in the following sections.

Finally, despite the effects of HDM exposure on metabolic parameters in both female and male mice, no differences in the respiratory quotient (RQ) were observed between groups. The RQ reflects substrate utilization for energy production, providing an indirect index of whether carbohydrates, lipids, or proteins are predominantly oxidized (Patel and Bhardwaj, 2023). Although HDM exposure altered other metabolic readouts, the preserved RQ suggests that the overall balance of substrate utilization remained stable across groups. This may indicate that allergen-induced airway inflammation affects metabolism without shifting the preferential energy substrate used under basal conditions.

4.3. HDM-induced airway inflammation alters ventilatory and metabolic responses to hypoxia in a sex-dependent manner

In the present study, we provide evidence of sex-specific alterations in the peripheral chemoreflex following HDM exposure in a murine model of airway inflammation. Specifically, males exposed to HDM presented an augmented hypoxic ventilatory response (HVR), whereas females appeared to exhibit a reduced one. In HDM-exposed males, the enhanced HVR was driven by increased f_R and V_E, along with reduced T_{insp}, T_{exp}, and cycle duration, indicating a faster breathing pattern during hypoxic exposure. Additionally, HDM-exposed males showed trends toward increased V_E/VO_2 ($p = 0.09$) and V_E/VCO_2 ($p =$

0.06), without changes in VO_2 or VCO_2, further supporting an enhanced chemoreflex drive to hypoxia following allergen exposure. Consistent with our findings, a recent study demonstrated an augmented HVR in ovalbumin (OVA)-sensitized male Brown Norway rats, which exhibited higher V_E/VO_2 and f_R during both moderate (12% O_2) and severe (9% O_2) hypoxia (Morgan et al., 2024).

In females, HDM exposure reduced T_{insp}, leading to a trend toward increased f_R ($p = 0.08$) after 10 minutes of hypoxia. However, f_R declined during the subsequent 10 minutes, suggesting a transient enhancement of HVR followed by a decrease during sustained hypoxia in this group. Interestingly, these females presented higher VO_2 and VCO_2 than controls during the same time point (20 min), while V_E remained unchanged. Because increased metabolic demand elevates CO_2 production and reduces O_2 availability during hypoxia, peripheral chemoreceptors would normally trigger a compensatory ventilatory response to match metabolic requirements. As this did not occur, HDM-exposed females showed a trend toward reduced V_E/VO_2 ($p = 0.09$), suggesting ventilatory–metabolic uncoupling and a hypoventilatory state, potentially due to a blunted carotid chemosensitivity following allergen exposure.

Hypoxia is classically associated with a coordinated reduction in metabolic rate as an energy-saving strategy (Gu and Jun, 2018; Mortola, 1993). Thus, the higher metabolism in HDM-exposed females compared with controls indicates an allergen-induced shift in metabolic adaptation to hypoxia. This may reflect disruptions in hypoxia-sensing pathways that normally promote energy conservation during low-oxygen exposure, such as AMP-activated protein kinase (AMPK) and hypoxia-inducible factor 1-alpha (HIF1-α) (Dengler, 2020). Indeed, reduced AMPK signaling and increased HIF-1α expression have been reported in the lungs of OVA-challenged female BALb/c mice, with HIF-1α also contributing to hypoxia-induced worsening of airway inflammation (Baek et al., 2013; Huerta-Yepez et al., 2011; Ma et al., 2022; Wan et al., 2024; Zhou et al., 2025). In inflammatory conditions, HIF-1α promotes metabolic reprogramming by stimulating glycolysis to sustain energetic demands, a hallmark of activated immune cells (Corcoran and O'Neill, 2016; Fitzpatrick et al., 2018; Gerriets et al., 2015; Sumbayev et al., 2010). Therefore, these potential alterations in hypoxia-sensing pathways may underlie the hypermetabolic response to hypoxia

following allergen exposure, possibly occurring specifically in females due to their higher pulmonary IL-5 levels compared with males.

Taken together, the current data support the hypothesis that allergic airway inflammation alters peripheral chemosensitivity in a sex-specific manner, enhancing HVR in males while reducing it in females. It has been proposed that proinflammatory mediators released from the lung may activate their receptors in type I glomus cells, modulating carotid chemoreception (Iturriaga et al., 2022; Porzionato et al., 2013). Consistent with this, IL-6 has found to increase intracellular calcium and catecholamine release in isolated rat type I cells, while Th2 cytokines (IL-4, IL-13, and eotaxin), non-Th2 cytokines (IL-1β, IL-6, and TNF-α), and lysophosphatidic acid increase oxygen-sensitive type I cells discharge in rat preparations (Fan et al., 2009; Jendzjowsky et al., 2018; 2021a; 2021b). In vivo, systemic administration of TNF-α increased carotid body afferent discharge and activated glutamatergic neurons in the nucleus tractus solitarius that project to the rostral ventrolateral medulla, increasing sympathetic activity (Katayama et al., 2022). However, when tested under hypoxic conditions, TNF-α reduced hypoxia-evoked discharge in isolated perfused carotid bodies, suggesting that this molecule impairs hypoxic chemosensitivity (Zapata et al., 2011).

Collectively, the available evidence indicates that inflammation may modulate carotid chemosensory function, either enhancing or suppressing it depending on the pre-existing stimulus, such as hypoxia. Moreover, sex hormones also play modulatory roles in the peripheral chemoreflex, with progesterone and testosterone described as classical respiratory stimulants during hypoxia (Janes et al., 2021; Joseph et al., 2013). Another potential mechanism through which sex hormones may influence carotid body chemosensitivity is via regulation of HIF-1α and HIF-2α expression. Indeed, a recent study showed that treatment of male and female rats with the estrogen metabolite 2-methoxyestradiol reduced HIF-1α expression in pulmonary artery smooth muscle cells (Docherty et al., 2019). In the carotid body, partial deletion of HIF-1α in mice leads to a blunted hypoxic chemoreflex, whereas partial deletion of HIF-2α results in exaggerated chemosensitivity (Kline et al., 2022; Peng et al., 2066; 2011). Therefore, these findings suggest that sex hormones

may differentially regulate HIF signaling pathways in the carotid body; however, direct evidence for this mechanism remains lacking.

The sex differences in the HVR following HDM exposure observed in our study highlight the importance of including both sexes in preclinical research, as this approach improves risk prediction and supports sex-specific clinical management strategies. For instance, we observed a hypoventilatory state due to hypermetabolic response during hypoxia in females, which potentially increases susceptibility to oxygen deprivation. This finding may be particularly relevant in women, as asthma has been associated with a higher risk of metabolic and cardiovascular comorbidities in female patients compared with men (Veenendaal et al., 2019; Wang et al., 2023). Conversely, the increased HVR in HDM-exposed males may predispose them to breathing instability via elevated loop gain, a hallmark in obstructive sleep apnea (Dempsey et al., 2014; Narkiewicz et al., 1998; 1999). This is especially noteworthy given that sleep apnea is more prevalent in adult men than in women and is also more frequently reported among individuals with asthma than among healthy subjects (Franklin and Lindberg, 2015; Kong et al., 2019; Lévy et al., 2015). Therefore, our data provides a novel framework for investigating asthma-associated comorbidities and suggests that HDM exposure in C57Bl/6 mice is a suitable model for exploring these pathways.

Finally, our data showed that sustained hypoxia decreased RQ after 20 minutes of exposure in control mice, due to a reduction in VCO_2 between 10 and 20 minutes of hypoxia. Although changes in RQ primarily reflect shifts in energy substrate utilization, the very low values of both RQ and VCO_2 observed during hypoxia indicate decreased metabolism as an adaptation to reduced oxygen availability (Gneiger et al., 2000). In parallel, in HDM-exposed mice, the reduction in RQ was accompanied by a marked increase in VO_2, suggesting an impaired mitochondrial adaptation to hypoxia following allergen exposure. Indeed, allergic asthma has been associated with mitochondrial dysfunction, including oxidative stress, impaired ATP production, alterations in oxidative phosphorylation, metabolic reprogramming, and reduced energetic efficiency (Qian et al., 2022). Therefore, our findings indicate that HDM-induced airway inflammation reduced

metabolic efficiency during hypoxia in both sexes, with this effect being more pronounced in females.

4.4. HDM-induced airway inflammation alters ventilatory and metabolic responses to hypercapnia in a sex-dependent manner

Regarding hypercapnic ventilatory response (HCVR), our data revealed decreased V_E/VO_2 in male mice exposed to HDM, particularly after 10 minutes of hypercapnic exposure. The attenuation in hipercanic hyperventilatory response was due to a higher metabolic demand (VO_2) without a proportional rise in V_E, despite elevated f_R across all hypercapnic challenges in HDM-exposed males compared with controls. The increase in f_R appears to represent a compensatory response attempt to match the elevated oxygen demand of this group, suggesting that the brainstem respiratory network remained partially responsive to both hypercapnic and metabolic stimuli after HDM exposure. In HDM-exposed females, a similar pattern was observed, but with no V_E/VO_2 changes.

These findings suggest that central chemoreflex pathways may have been modulated by allergen exposure. Indeed, accumulating evidence indicates that inflammatory mediators in the airways activate sensory neurons innervating the airways, alveoli, and airway smooth muscle, enhancing vagal afferent signaling to the nucleus tractus solitarius (NTS) (Spaziano et al., 2015; Su et al., 2024; Zhu et al., 2026). Therefore, given its role in central chemoreflex processing and its projections to chemosensory nuclei, including the retrotrapezoid nucleus (RTN) and locus coeruleus (LC), inflammation-induced activation of the NTS may modulate chemosensitive neurons' activity and alter HCVR (Guyenet et al., 2019; Lopes et al., 2016).

If this hypothesis is correct, NTS neurons receiving bronchopulmonary vagal inputs, particularly those activated by inflammatory stimuli, may project to brainstem chemosensory nuclei. Indeed, vagal afferents from the lungs and airways terminate predominantly within the medial and caudal subdivisions of the NTS, and projections to LC arise primarily from neurons located within the caudal NTS, particularly its commissural subdivision (Van Bockstaele et al., 1999; Kawai, 2018; Kubin et al., 2006). In addition, second-order NTS neurons activated by pulmonary slowly adapting receptors (SARs) provide excitatory glutamatergic

input to the noradrenergic A5 cell group; however, there is no evidence that SARs are activated by inflammatory stimuli in the airways (Ezurek et al., 1998). Moreover, a recent study using anterograde viral tracing in rats provided evidence of multiple sensory circuits originating from the trachea and lungs to the LC, although the type of these sensory neurons was not described (McGovern et al., 2015). Vagal C-fiber afferents are considered the primary bronchopulmonary sensory pathway responsive to inflammatory mediators in asthma, and there is no evidence of direct afference to LC or RTN (Undem and Taylor-Clark, 2014).

Given that f_R was enhanced, another potentially involved component is excitatory input from chemosensory regions, such as the RTN and LC, to the respiratory rhythm-generating network, including the pre-Bötzinger complex (preBötC) (Hernandez-Miranda and Birchmeier, 2015; Liu et al., 2021). Indeed, HDM-exposed males and females exhibited higher f_R than controls during hypercapnia, driven by reduced T_{insp} and T_{exp} in males and females, respectively. Interestingly, basal f_R in HDM-exposed males was similar to that of controls but remained elevated following the respiratory challenge due to lower T_{insp}, suggesting that allergen exposure primed the rhythm-generating center to respond more strongly during and after a respiratory challenge. Because the order of hypoxic and hypercapnic exposures was alternated among animals, our data does not allow us to identify which stimulus primarily triggered the allergen exposure effect.

The increased VO_2 observed in HDM-exposed mice of both sexes during hypercapnia may reflect the elevated cost of breathing under pathological conditions (O'Donnell et al., 2002). This is consistent with the well-established relationship between ventilatory work and respiratory muscle VO_2, which can account for a substantial fraction of total VO_2 during states of increased ventilatory demand, especially hypercapnia (Aaron et al., 1992; Coast et al., 1993; Ostergaard et al., 2012). In obstructive diseases, mechanical limitation further increases the work of breathing by recruiting accessory respiratory muscles (O'Donnell et al., 2002; Scano et al., 2006). In parallel, asthma-related inflammatory mediators alter pulmonary energetic homeostasis by increasing tissue oxygen requirements, thereby elevating the metabolic cost of ventilation under hypercapnic conditions (Felton et al., 2014; Fulkerson and Rothenberg,

2013; Koranteng et al., 2024; Porter et al., 2018). Collectively, these mechanisms may account for a higher VO_2 in HDM-exposed mice during hypercapnia, particularly in the first 10 minutes of exposure.

Taken together, our findings suggest that, in males exposed to HDM, central chemosensitivity remained at least partially responsive, as evidenced by the increase in f_R during hypercapnia. However, it was insufficient to match the elevated metabolic demand, resulting in reduced hyperventilatory response. It is noteworthy that the HCVR depends on coordinated increases in both V_T and f_R (Biancardi et al., 2008). However, whereas f_R was higher in HDM-exposed males, V_T was the same compared with controls. It is possible that V_T failed to increase due to reduced chemoreflex following allergen exposure; however, we cannot exclude possible mechanical impairments resulting from airway inflammation (Rojas-Ruiz et al., 2024). Thus, the decreased CO_2-hyperventilatory response of HDM-exposed males may reflect a partial blunted central chemoreception or a combination of metabolic dysfunction with mechanical limitations. Nevertheless, the persistence of tachypneic breathing during recovery indicates that respiratory rhythm-generating circuits may have been facilitated by HDM exposure in males. Indeed, f_R was higher in HDM-exposed males also during hypoxia. These findings suggest that shared components of the peripheral and central chemoreflex pathways, including preBötC, were sensitized to allergen exposure in males.

Similarly, the increase in f_R observed in HDM-exposed females during hypercapnia was accompanied by an increased VO_2; however, it was insufficient to prevent the reduced hyperventilatory response. It is worth noting that HDM-exposed females showed a tendency toward increased V_E/VCO_2 during the first 10 minutes of hypercapnia; however, it returned to control levels after 20 minutes of exposure. Therefore, our data do not allow us to determine whether the increased f_R observed in HDM-exposed females during hypercapnia reflects enhanced central chemosensitivity or preserved respiratory circuitry responding appropriately to the increased metabolic demand induced by allergen exposure.

Finally, our data showed a reduction in RQ in both control and HDM-exposed male and female mice after 10 min of hypercapnia compared with baseline, reaching values nearly 0.7, consistent with a transient shift toward lipid utilization (Patel and Bhardwaj, 2023). This decrease was more pronounced in

HDM-exposed females, largely due to their higher VO_2 relative to controls. In contrast, although HDM-exposed males showed increased VO_2, RQ did not differ between groups. After 20 min of hypercapnia, RQ increased similarly across all groups, then returned to values close to baseline (~0.8) due to increased VCO_2 without changes in VO_2. This suggests a progressive restoration of the balance between VCO_2 and VO_2 as adaptation to hypercapnia occurred. These findings indicate that the initial metabolic shift induced by hypercapnia was transient in all groups but was amplified by allergen exposure in females; however, sustained hypercapnia did not result in persistent alterations in substrate utilization, regardless of sex or allergen exposure.

Collectively, our data highlight an important sex-specific HCVR following airway inflammation, with males exhibiting a reduced ability to match ventilation to the metabolic demands during hypercapnia. This reduced hyperventilatory response in HDM mice may promote CO_2 retention, thereby increasing susceptibility to its deleterious effects, including enhanced airway smooth muscle contraction, impaired innate immune responses, and increased adipogenesis (Casalino-Matsuda et al., 2020; Fitzpatrick et al., 2008; Kikuchi et al., 2017; Shigemura et al., 2018). These effects are particularly relevant in asthma, as respiratory infections are major triggers of exacerbations, and obesity is a risk factor for obstructive sleep apnea in asthmatic patients (Barros et al, 2017; Iikura et al., 2015; Kong et al., 2017; Resiliac and Greyson, 2019). Therefore, although hypercapnia is often associated with severe airway obstruction in asthma, our findings suggest that alterations in chemoreflex pathways may also contribute to its development, particularly in males (Scala, 2010; Shigemura et al., 2020).

The sex differences observed in the HCVR following allergen exposure may be explained not only by the influence of sex hormones on the hypercapnic response, which remains controversial in the literature, but also by sexual dimorphism in central chemosensitive regions (Gargaglioni et al., 2019). Immunohistochemical analyses have shown that female C57Bl/6 mice have fewer noradrenergic neurons in the LC but exhibit greater dendritic volume than males (Mariscal et al., 2023). In addition, patch-clamp electrophysiological studies have demonstrated that LC neurons from female mice are intrinsically more excitable than those from males, despite exhibiting similar action potential

properties (Mariscal et al., 2023). With respect to the RTN, exposure to 5% CO_2 induced greater neuronal activation in male transgenic mice with a c-Fos promoter drive, whereas females displayed a higher number of activated cells in the rostral medulla (Niblock et al., 2010). Collectively, these findings raise the possibility that the chemosensory nuclei may exhibit sex-specific sensitivities to CO_2 and recruit neuronal populations in distinct intensities. Because central chemoreflex processing involves multiple nuclei, further studies are needed to clarify the sex-specific effects of airway inflammation on that pathway in mice (Forster and Smith, 2010; Ikeda et al., 2017).

5. CONCLUSON

Taken together, our findings suggest that HDM-induced allergic inflammation promotes sex-dependent alterations in basal metabolism, particularly by reducing oxygen consumption in females. In addition, it differentially modulates hypoxic chemosensitivity, enhancing it in males while attenuating it in females. Finally, HDM exposure also alters hypercapnic chemosensitivity in a sex-dependent manner, leading to a reduced response in males.

6. REFERENCES

Aun MV, et al. Animal models of asthma. J Asthma Allergy, 10, p. 293-301, 2017.

Bailey JE, et al. Does the brain noradrenaline network mediate the effects of the CO2 challenge? J Psychopharmacol, 17, p. 252-259, 2003.

Biancardi V, et al. Locus coeruleus noradrenergic neurons and CO2 drive to breathing. Pflugers Arch, 455, p. 1119-1128, 2008.

Blain GM, Smith CA, Henderson KS, Dempsey JA. Peripheral chemoreceptors determine the respiratory sensitivity of central chemoreceptors to CO2. J Physiol, 588, p. 2455-2471, 2010.

Brinkman JE, Sharma S. Physiology, Respiratory Drive. StatPearls, p. 1-1, 2018.

Carroll OR, et al. Advances in respiratory physiology in mouse models of asthma. Front Physiol, 14, p. 1099719, 2023.

Conrad SC, et al. Development of chemosensitivity in neurons from the nucleus tractus solitarii. Respir Physiol Neurobiol, 166, p. 4-12, 2009.

Cooper CL, et al. Anxiety and panic fear in adults with asthma. BMC Fam Pract, 8, p. 62, 2007.

Cosgrove JF, et al. The ventilatory response to carbon dioxide in asthmatic children. Pediatrics, 57, p. 952-959, 1976.

Dempsey JA, Gibbons TD. Rethinking O2, CO2 and breathing. J Physiol, 602, p. 5571-5585, 2024.

Favreau H, et al. Panic disorder and asthma control. Psychosom Med, 76, p. 147-155, 2014.

Franklin KA, Lindberg E. Obstructive sleep apnea is a common disorder in the population-a review on the epidemiology of sleep apnea. J Thorac Dis, 7(8), p. 1311-1322, 2015.

Gargaglioni LH, et al. The locus coeruleus and central chemosensitivity. Respir Physiol Neurobiol, 173, p. 264-273, 2010.

Gibson GJ. Perception, personality, and respiratory control in life-threatening asthma. Thorax, 50, p. S2-S4, 1995.

Goodwin RD, et al. Asthma and mental disorders in Canada. J Psychosom Res, 68, p. 165-173, 2010.

Gregory LG, Lloyd CM. Orchestrating house dust mite-associated allergy. Trends Immunol, 32, p. 402-411, 2011.

Griez E, Schruers K. Mechanisms of CO2 challenges. J Psychopharmacol, 17, p. 267-268, 2003.

Guner I, et al. Intracerebroventricular serotonin reduces the degree of acute hypoxic ventilatory depression in peripherally chemodenervated rabbits. Chin J Physiol, 51, p. 136-145, 2008.

Hasler G, et al. Asthma and panic in young adults. Am J Respir Crit Care Med, 171, p. 1224-1230, 2005.

Hernandez-Miranda LR, Birchmeier C. CO2 in the spotlight. Elife, 4, p. e08086, 2015.

Hida W. Papel do estímulo ventilatório na asma e na doença pulmonar obstrutiva crônica. Current Opinion in Pulmonary Medicine, 5, p. 339, 1999.

Hida W. Role of ventilatory drive in asthma and chronic obstructive pulmonary disease. Curr Opin Pulm Med, 5, p. 339, 1999.

Hudgel DW, Weil JV. Depression of hypoxic and hypercapnic ventilatory drives in severe asthma. Chest, 68, p. 493-497, 1975.

Hutchison AA, Olinsky A. Hypoxic and hypercapnic response in asthmatic subjects. Thorax, 36, p. 759-763, 1981.

Ikeda K, Kawakami K, Onimaru H, Okada Y, Yokota S, et al. The respiratory control mechanisms in the brainstem and spinal cord: integrative views of the neuroanatomy and neurophysiology. J Physiol Sci, 67, p. 45-62, 2017.

Jendzjowsky NG, et al. Asthmatic allergen inhalation sensitises carotid bodies. J Neuroinflammation, 18, p. 191, 2021.

Kamra K, Xia Z, Zucker IH, Schultz H, Wang HJ. Chemoreflex function in pulmonary diseases - A review. J Physiol, 603, p. 4461-4482, 2025.

Katayama PL, et al. The carotid body detects TNF-alpha. Brain Behav Immun, 102, p. 370-386, 2022.

Kelsen S, Fleegler B, Altose M. The respiratory neuromuscular response to hypoxia, hypercapnia, and obstruction in asthma. Am Rev Respir Dis, 120, p. 517-527, 1979.

Kikuchi Y, et al. Chemosensitivity and perception of dyspnea in near-fatal asthma. N Engl J Med, 330, p. 1329-1334, 1994.

Klein DF. False suffocation alarms and spontaneous panic. Arch Gen Psychiatry, 50, p. 306-317, 1993.

Kong DL, et al. Association of OSA with asthma. Sci Rep, 7, p. 4088, 2017.

Lavoie KL, et al. Psychiatric disorders and asthma control. Respir Med, 99, p. 1249-1257, 2005.

Lévy P, et al. Obstructive sleep apnoea syndrome. Nat Rev Dis Primers, 1:15015, 2015.

Li A, Nattie EE. Catecholamine neurons in rats modulate sleep, breathing. 2006.

Morgan BJ, et al. Altered control of breathing in allergic airway inflammation. J Neurophysiol, 132, p. 1650-1666, 2024.

Munakata M, et al. Female asthmatics have increased hypercapnic chemosensitivity. Chest, 104, p. 1718-1722, 1993.

Nattie E, Li A. Central chemoreceptors: locations and functions. Compr Physiol, p. 221-254, 2012.

Olaya B et al. Epidemiology of panic attacks, panic disorder and the moderating role of age: Results from a population-based study. J Affect Disord, 1, 241, p. 627-633, 2018.

Pichard LE, et al. Role of BK Channels in Murine Carotid Body Neural Responses in vivo. Adv Exp Med Biol, 860, p. 325-333, 2015.

Rebuck AS, Read J. Patterns of ventilatory response to carbon dioxide during recovery from severe asthma. Clin Sci, 41, p. 13-21, 1971.

Ritucci NA, et al. Response of membrane potential and intracellular pH to hypercapnia in neurons. Am J Physiol Regul Integr Comp Physiol, 289, p. R851-R861, 2005.

Smith TF, Hudgel DW. Decreased ventilation response to hypoxia in children with asthma. J Pediatr, 97, p. 736-741, 1980.

Su Y, et al. Brainstem Dbh+ neurons control allergen-induced airway hyperreactivity. Nature, 631, p. 601-609, 2024.

Sundbom F, et al. Asthma and asthma-related comorbidity: effects on nocturnal oxygen saturation. J Clin Sleep Med, 18(11), p. 2635-2641, 2022.

Takakura AC, et al. Peripheral chemoreceptor inputs to retrotrapezoid nucleus (RTN) CO2 sensitive neurons in rats. J Physiol, 572, p. 503-523, 2006.

Taneja P, et al. Pathophysiology of locus coeruleus neurons in a mouse model of Rett syndrome. J Neurosci, 29, p. 12187-12195, 2009.

Teodorescu M, et al. Asthma and risk of obstructive sleep apnea. JAMA, 313, p. 156-164, 2015.

Town G, Allan C. Ventilatory responses to hypoxia and hypercapnia in asthmatics. Aust N Z J Med, 19, p. 426-430, 1989.

Valdes B et al. Recognition and Treatment of Psychiatric Emergencies for Health Care Providers in the Emergency Department: Panic Attack, Panic Disorder, and Adverse Drug Reactions. J Emerg Nurs, 47(3), p. 459-468, 2021.

Vollmer LL, et al. Microglial acid sensing regulates CO2-evoked fear. Biol Psychiatry, 80, p. 541-551, 2016.

Wang D, et al. Association between ventilatory response to hypercapnia and OSA. Sleep Breath, 11, p. 103-108, 2007.

Wang D, et al. Ventilatory response to hypercapnia in OSA. Sleep Breath, 11, p. 103-108, 2007.

Wang W, et al. Chemosensitivity of rat medullary raphe neurones in culture. J Physiol, 511, p. 433-450, 1998.

Wemmie JA. The amygdala regulates CO2-evoked fear. Behav Brain Res, 377, p. 112236, 2019.

Woodrow JS, et al. Asthma: animal models and translational utility. Cells, 12, p. 1091, 2023.

Xu F, et al. Ovalbumin sensitization alters ventilatory responses. J Appl Physiol, 99, p. 1782-1788, 2005.

Ziemann AE, et al. The amygdala is a chemosensor that detects carbon dioxide and acidosis. Cell, 139, p. 1012-1021, 2009.

Figure legends

Figure 1: Schematic illustration of study desing. Created with Biorender; License LHG.

Figure 2: Effect of HDM exposure on total BALF cell counts (A) and differential BALF cell counts expressed as a percentage of 300 cells (B) in both female and male mice. * Represents significant differences between HDM and control groups ($p < 0.05$).

Figure 3: Representative photomicrographs of lung sections stained with H&E (Ai, Aii) and PAS (Aiii, Aiv) from control and HDM groups. Objective magnification of 20x (Ai, Aii, Aiii, Aiv). Asterisks (*) indicate airways, and black arrows indicate blood vessels. Effect of HDM exposure on peribronchial inflammation score (B), perivascular inflammation score (C) and PAS score (D). * Represents significant differences between HDM and control groups ($p < 0.05$).

Figure 4: Effect of HDM exposure on plasma IL-13 levels (A), BALF IL-13 levels (B), lung IL-4 levels (C), lung IL-5 levels (D), and lung IL-13 levels (E) in both female and male mice. * Represents significant differences between HDM and control groups ($p < 0.05$). + Represents significant differences between male and female within the same group ($p < 0.05$).

Figure 5: Effect of HDM exposure on BALF IL-13 levels (A), lung IL-4 levels (B), lung IL-5 levels (C), and lung IL-13 levels (D) in both female and male mice from experiment 3.

Figure 6: Effect of HDM exposure on tidal volume (V_T; A), respiratory frequency (f_R; B), ventilation (V_E; C), inspiration time (T_{insp}; D), expiration time (T_{exp}; E), cycle duration (CD; F); oxygen consumption (VO_2; G); CO_2 production (VCO_2; H); respiratory quotient (RQ; I); ventilatory equivalent for O_2 (V_E/VO_2; J), ventilatory equivalent for CO_2 (V_E/VCO_2; K), and body temperature (T_B; L) in female mice during baseline and recovery under room air conditions. * Represents significant diferences between HDM and control groups ($p < 0.05$). # Represents significant differences between baseline and recovery within the same group ($p < 0.05$).

Figure 7: Effect of HDM exposure on tidal volume (V_T; A), respiratory frequency (f_R; B), ventilation (V_E; C), inspiration time (T_{insp}; D), expiration time (T_{exp}; E), cycle

duration (CD; F); oxygen consumption (VO_2; G); CO_2 production (VCO_2; H); respiratory quotient (RQ; I); ventilatory equivalent for O_2 (V_E/VO_2; J), ventilatory equivalent for CO_2 (V_E/VCO_2; K), and body temperature (T_B; L) in male mice during baseline and recovery under room air conditions. * Represents significant differences between HDM and control groups ($p < 0.05$). # Represents significant differences between baseline and recovery within the same group ($p < 0.05$).

Figure 8: Effect of HDM exposure on tidal volume (V_T; A), respiratory frequency (f_R; B), ventilation (V_E; C), inspiration time (T_{insp}; D), expiration time (T_{exp}; E), cycle duration (CD; F); oxygen consumption (VO_2; G); CO_2 production (VCO_2; H); respiratory quotient (RQ; I); ventilatory equivalent for O_2 (V_E/VO_2; J), ventilatory equivalent for CO_2 (V_E/VCO_2; K), and body temperature (T_B; L) in female mice during hypoxic conditions. * Represents significant differences between HDM and control groups ($p < 0.05$). # Represents significant differences between 10 minutes and 20 minutes within the same group ($p < 0.05$).

Figure 9: Effect of HDM exposure on tidal volume (V_T; A), respiratory frequency (f_R; B), ventilation (V_E; C), inspiration time (T_{insp}; D), expiration time (T_{exp}; E), cycle duration (CD; F); oxygen consumption (VO_2; G); CO_2 production (VCO_2; H); respiratory quotient (RQ; I); ventilatory equivalent for O_2 (V_E/VO_2; J), ventilatory equivalent for CO_2 (V_E/VCO_2; K), and body temperature (T_B; L) in male mice during hypoxic conditions. * Represents significant differences between HDM and control groups ($p < 0.05$). # Represents significant differences between 10 minutes and 20 minutes within the same group ($p < 0.05$).

Figure 10: Effect of HDM exposure on tidal volume (V_T; A), respiratory frequency (f_R; B), ventilation (V_E; C), inspiration time (T_{insp}; D), expiration time (T_{exp}; E), cycle duration (CD; F); oxygen consumption (VO_2; G); CO_2 production (VCO_2; H); respiratory quotient (RQ; I); ventilatory equivalent for O_2 (V_E/VO_2; J), ventilatory equivalent for CO_2 (V_E/VCO_2; K), and body temperature (T_B; L) in female mice during hypercapnic conditions. * Represents significant diferences between HDM and control groups ($p < 0.05$). # Represents significant diferences between 10 minutes and 20 minutes whithin the same group ($p < 0.05$).

Figure 11: Effect of HDM exposure on tidal volume (V_T; A), respiratory frequency (f_R; B), ventilation (V_E; C), inspiration time (T_{insp}; D), expiration time (T_{exp}; E), cycle

duration (CD; F); oxygen consumption (VO_2; G); CO_2 production (VCO_2; H); respiratory quotient (RQ; I); ventilatory equivalent for O_2 (V_E/VO_2; J), ventilatory equivalent for CO_2 (V_E/VCO_2; K), and body temperature (T_B; L) in male mice during hypercapnic conditions. * Represents significant diferences between HDM and control groups ($p < 0.05$). # Represents significant diferences between 10 minutes and 20 minutes whithin the same group ($p < 0.05$).

Figures

Figure 1.

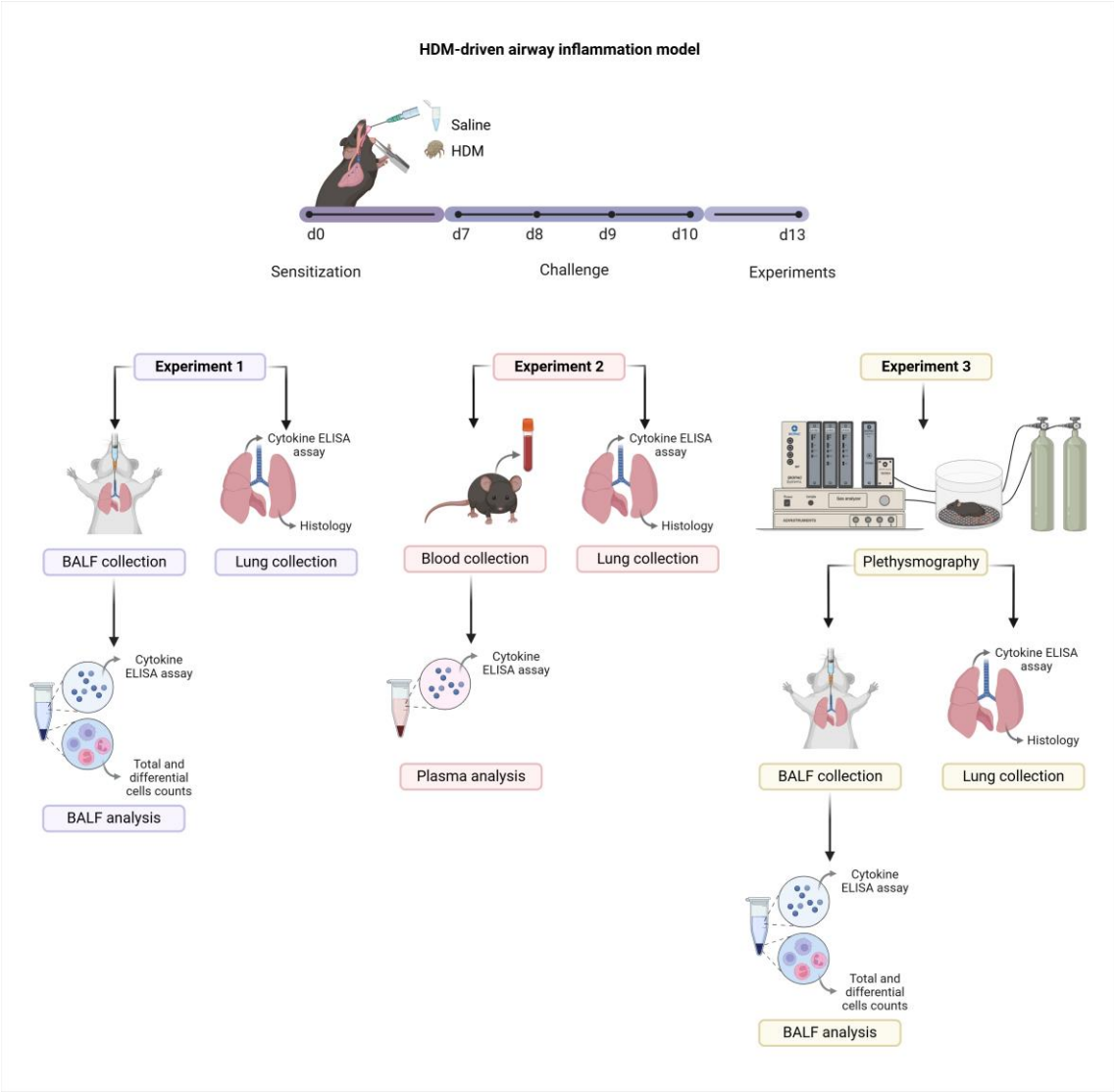

Figure 2.

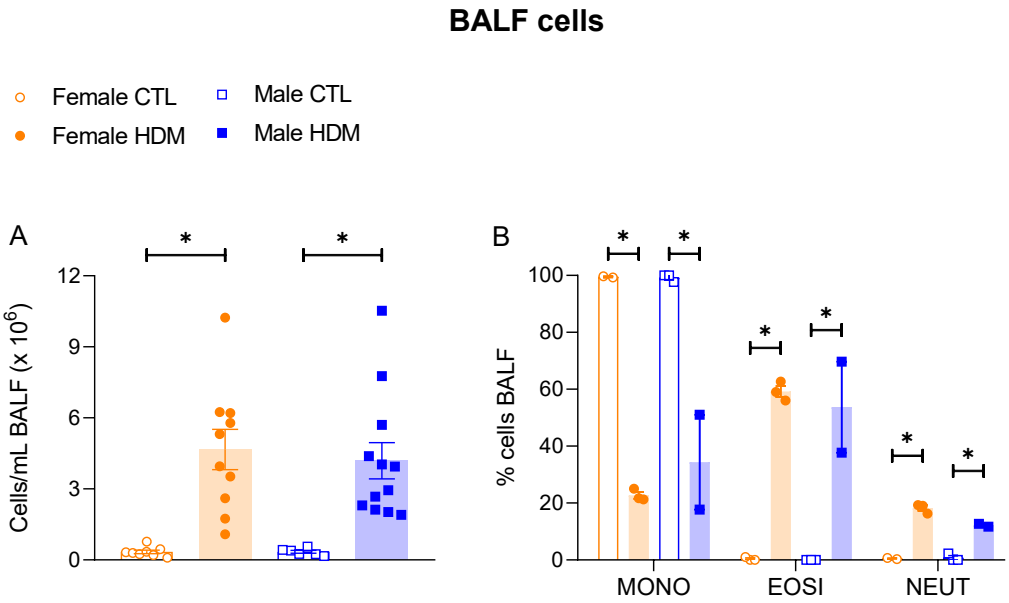
BALF cells
Female CTL
Female HDM
Male CTL
Male HDM
A
Cells/mL BALF (x 10^6)
12
9
6
3
0
*
*
B
% cells BALF
100
80
60
40
20
0
*
*
*
*
*
*
MONO
EOSI
NEUT

Figure 3.

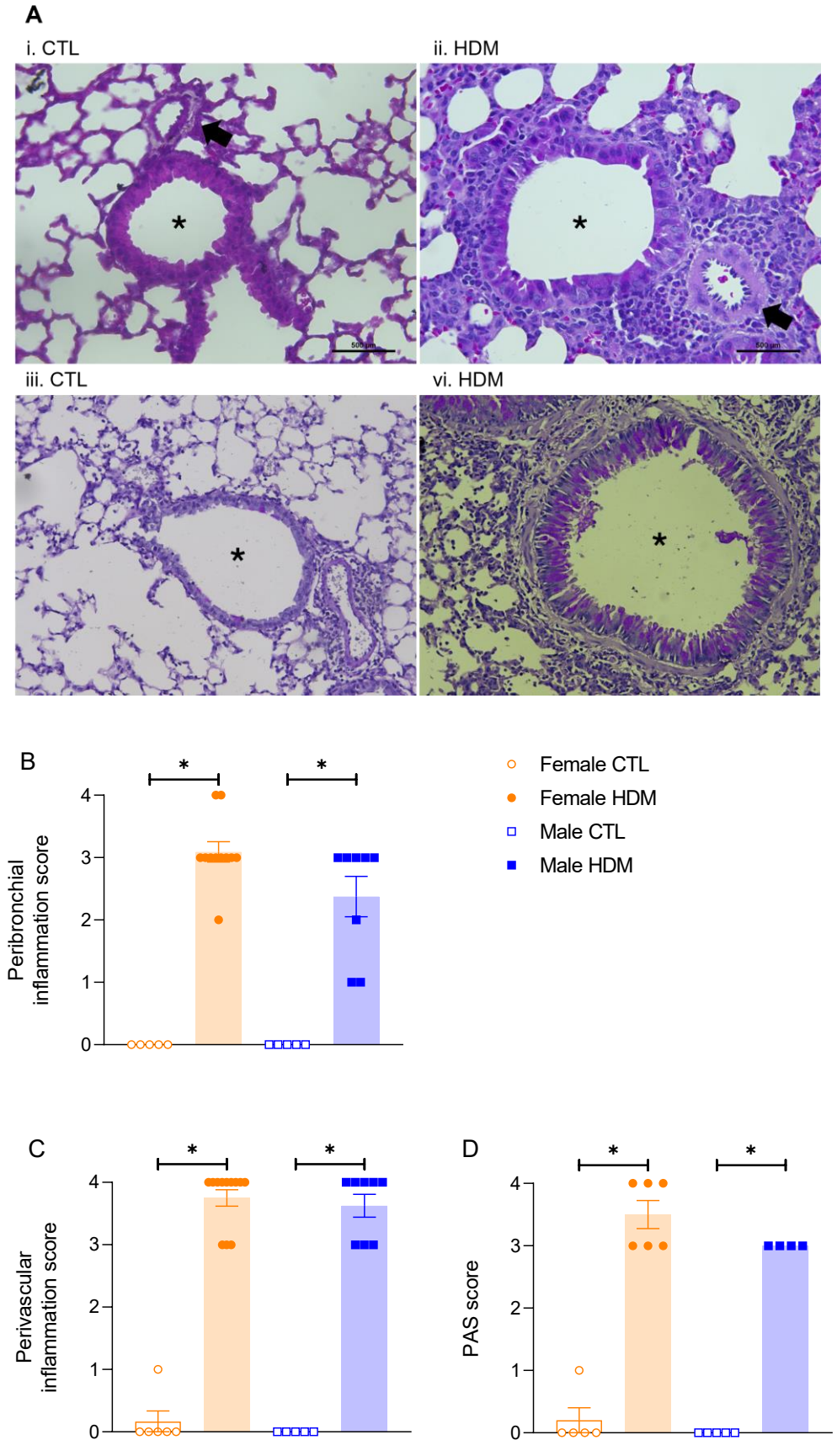
A
i. CTL
ii. HDM
iii. CTL
vi. HDM
B
Peribronchial inflammation score
Female CTL
Female HDM
Male CTL
Male HDM
C
Perivascular inflammation score
D
PAS score

Figure 4.

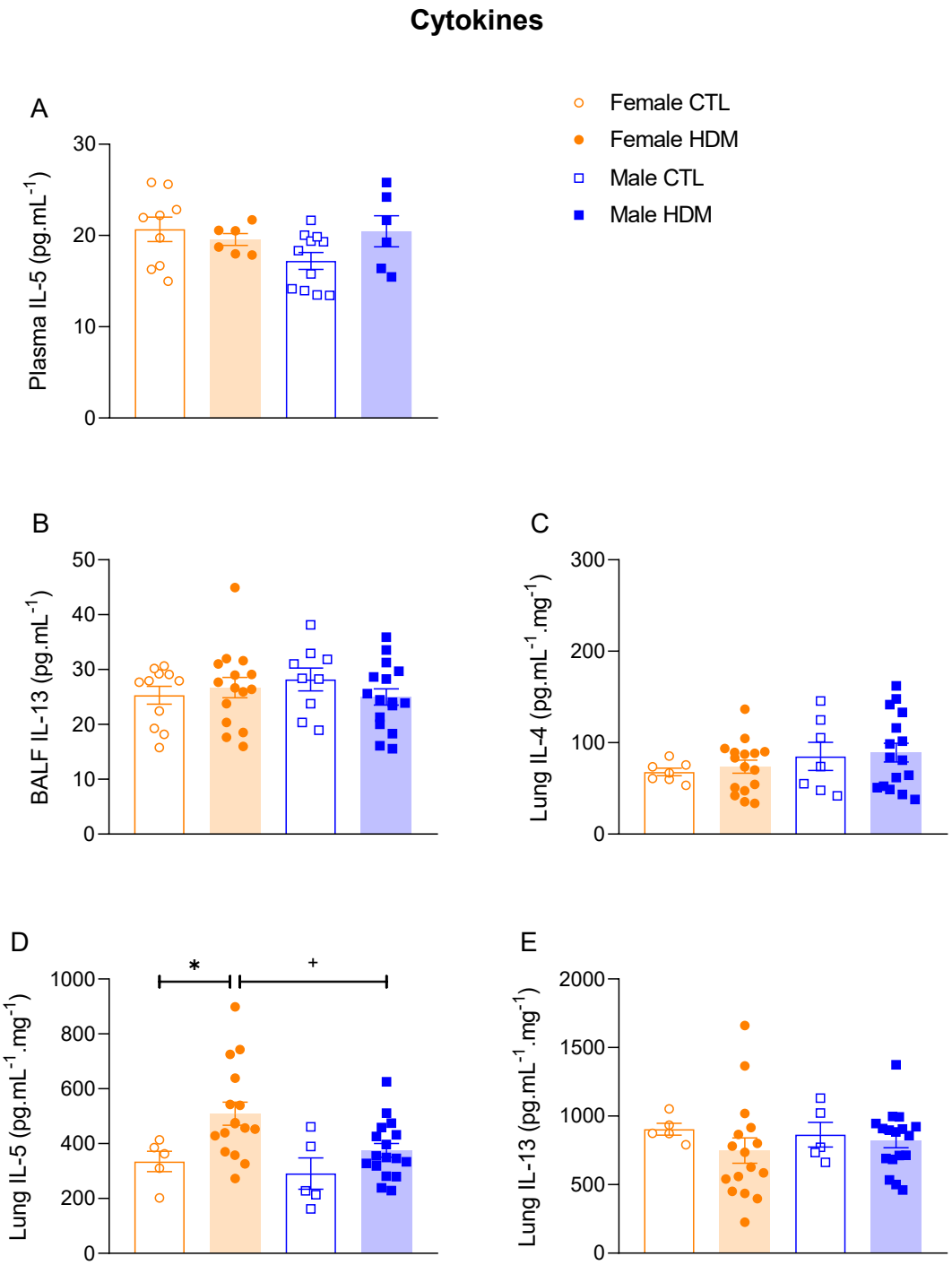
Cytokines
A
Plasma IL-5 (pg.mL-1)
30
20
10
0
Female CTL
Female HDM
Male CTL
Male HDM
B
BALF IL-13 (pg.mL-1)
50
40
30
20
10
0
C
Lung IL-4 (pg.mL-1.mg-1)
300
200
100
0
D
Lung IL-5 (pg.mL-1.mg-1)
1000
800
600
400
200
0
*
+
E
Lung IL-13 (pg.mL-1.mg-1)
2000
1500
1000
500
0

Figure 5.

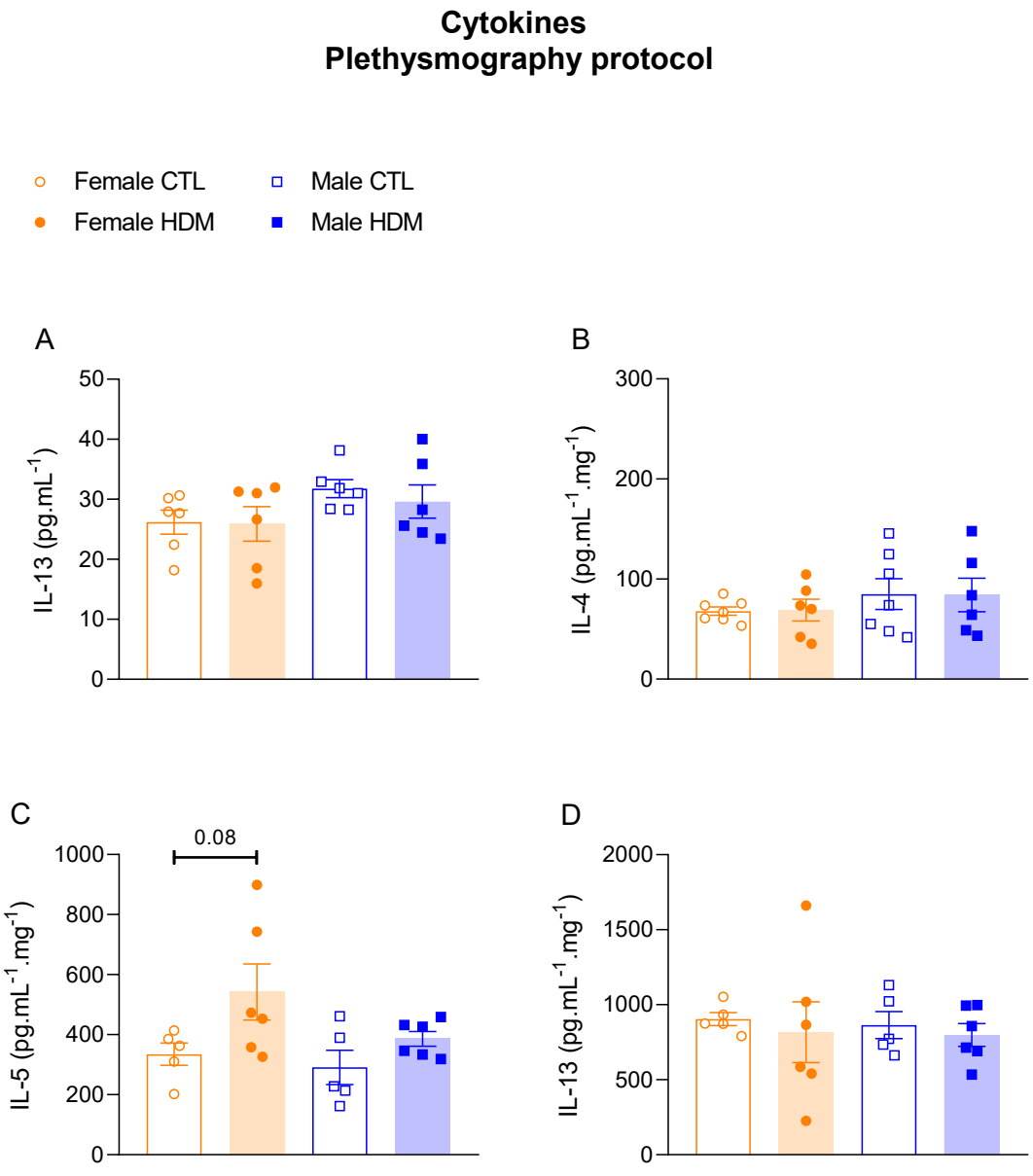
Cytokines
Plethysmography protocol
Female CTL
Female HDM
Male CTL
Male HDM
A
IL-13 (pg.mL-1)
50
40
30
20
10
0
B
IL-4 (pg.mL-1.mg-1)
300
200
100
0
C
IL-5 (pg.mL-1.mg-1)
0.08
1000
800
600
400
200
0
D
IL-13 (pg.mL-1.mg-1)
2000
1500
1000
500
0

Figure 6.

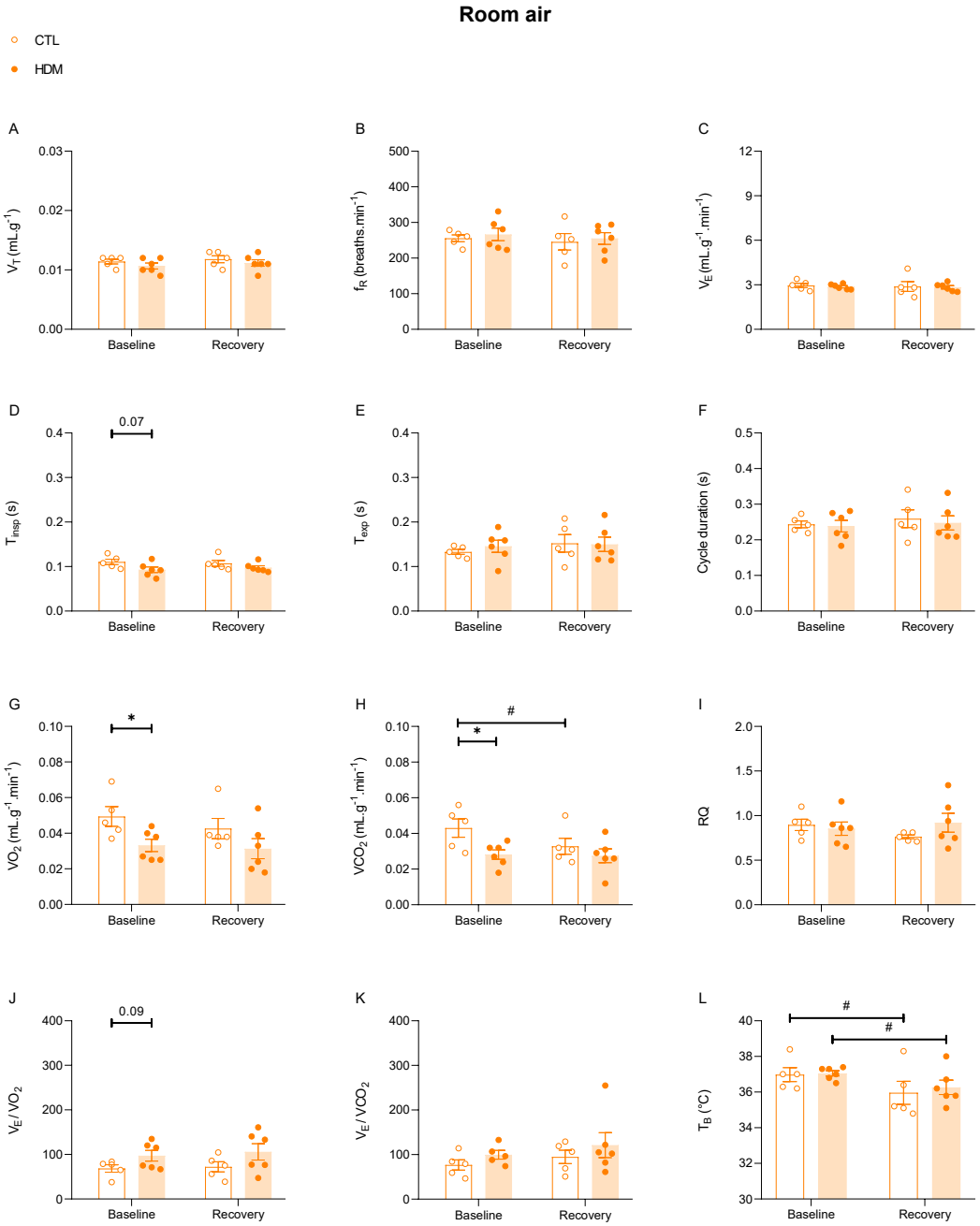
Room air
CTL
HDM
A
V_T (mL.g^{-1})
B
f_R (breaths.min^{-1})
C
V_E (mL.g^{-1}.min^{-1})
D
0.07
T_{insp} (s)
E
T_{exp} (s)
F
Cycle duration (s)
G
*
VO_2 (mL.g^{-1}.min^{-1})
H
#
*
VCO_2 (mL.g^{-1}.min^{-1})
I
RQ
J
0.09
V_E/VO_2
K
V_E/VCO_2
L
#
#
T_B (°C)
Baseline
Recovery

Figure 7.

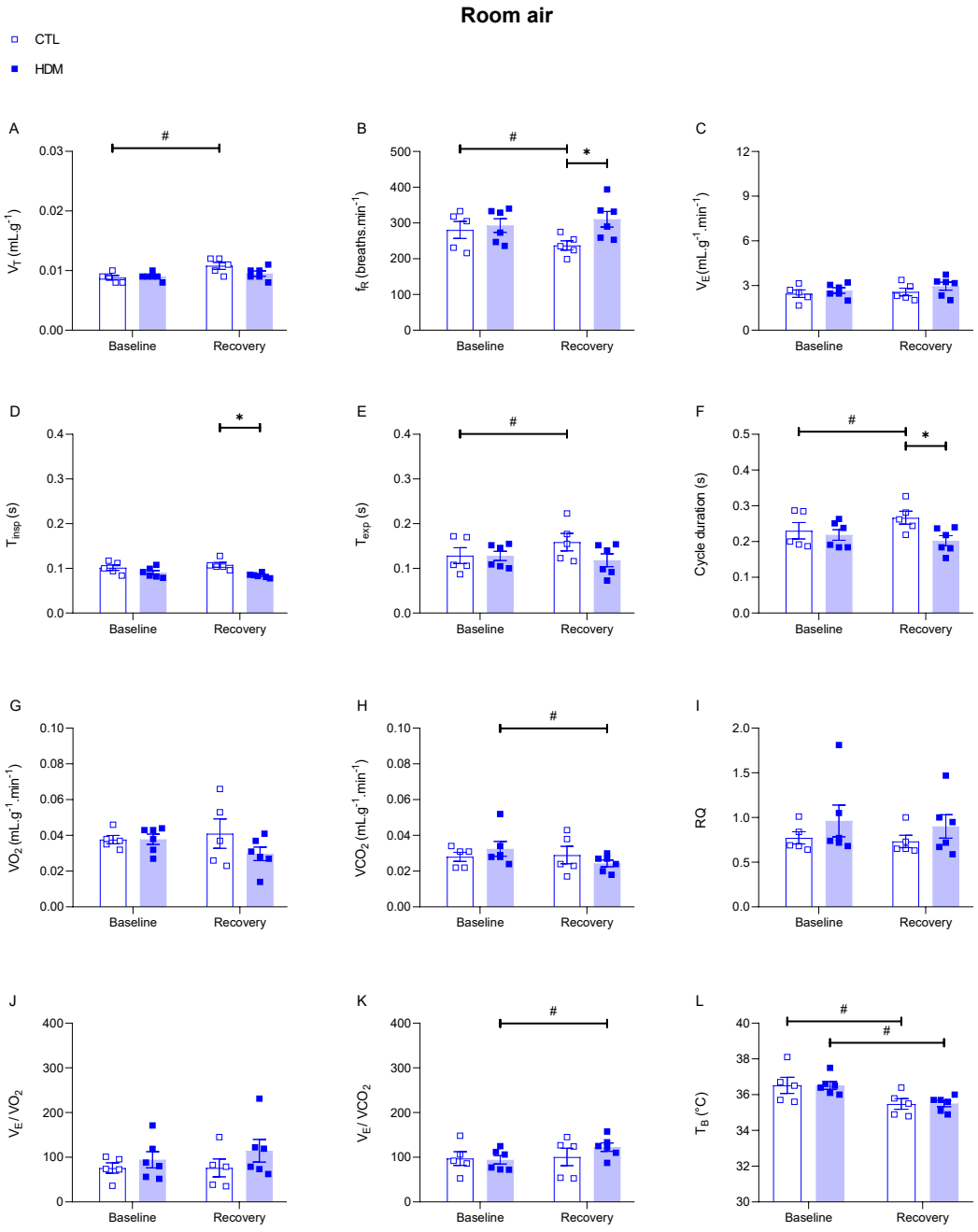

Figure 8.

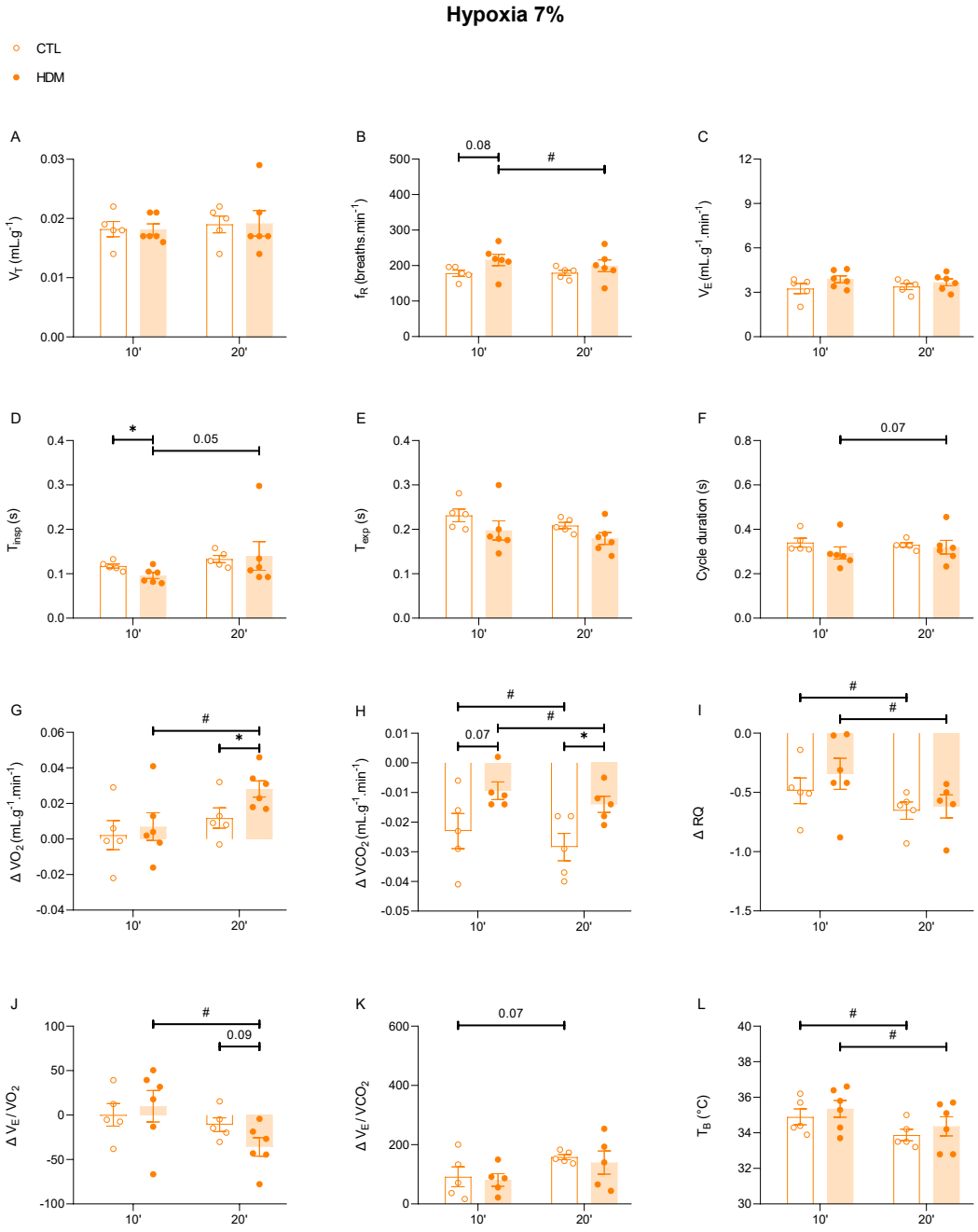
Hypoxia 7%
CTL
HDM
A
B
C
D
E
F
G
H
I
J
K
L
V_T (mL.g^{-1})
f_R (breaths.min^{-1})
V_E(mL.g^{-1}.min^{-1})
T_{insp} (s)
T_{exp} (s)
Cycle duration (s)
Δ VO_2(mL.g^{-1}.min^{-1})
Δ VCO_2(mL.g^{-1}.min^{-1})
Δ RQ
Δ V_E/VO_2
Δ V_E/VCO_2
T_B (°C)
10'
20'
0.08
0.05
0.07
0.09
#
*

Figure 9.

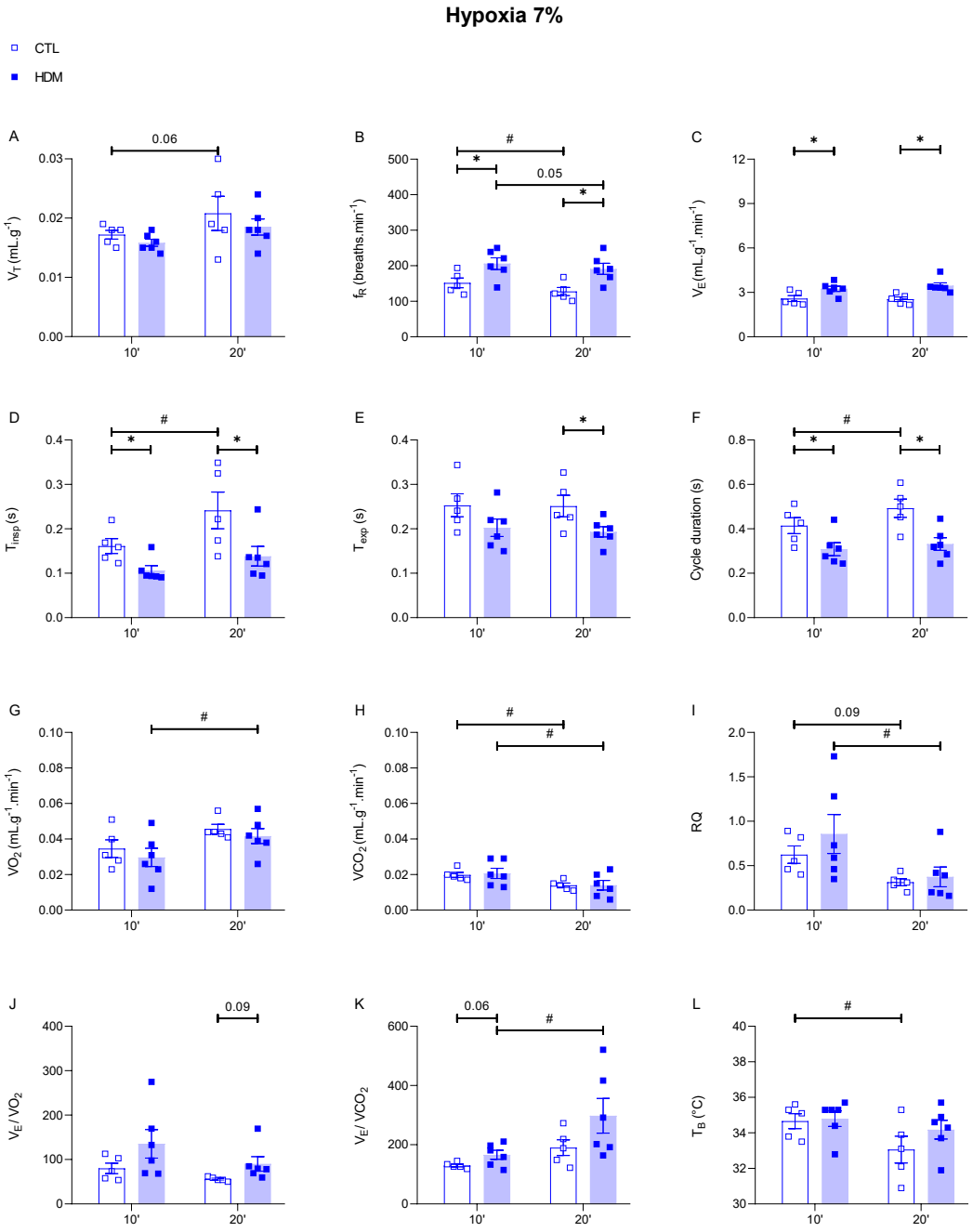
Hypoxia 7%
CTL
HDM
A
B
C
D
E
F
G
H
I
J
K
L
0.06
0.05
0.09
#
*
10'
20'
V_T (mL.g^{-1})
f_R (breaths.min^{-1})
V_E (mL.g^{-1}.min^{-1})
T_{insp} (s)
T_{exp} (s)
Cycle duration (s)
VO_2 (mL.g^{-1}.min^{-1})
VCO_2 (mL.g^{-1}.min^{-1})
RQ
V_E/ VO_2
V_E/ VCO_2
T_B (°C)

Figure 10.

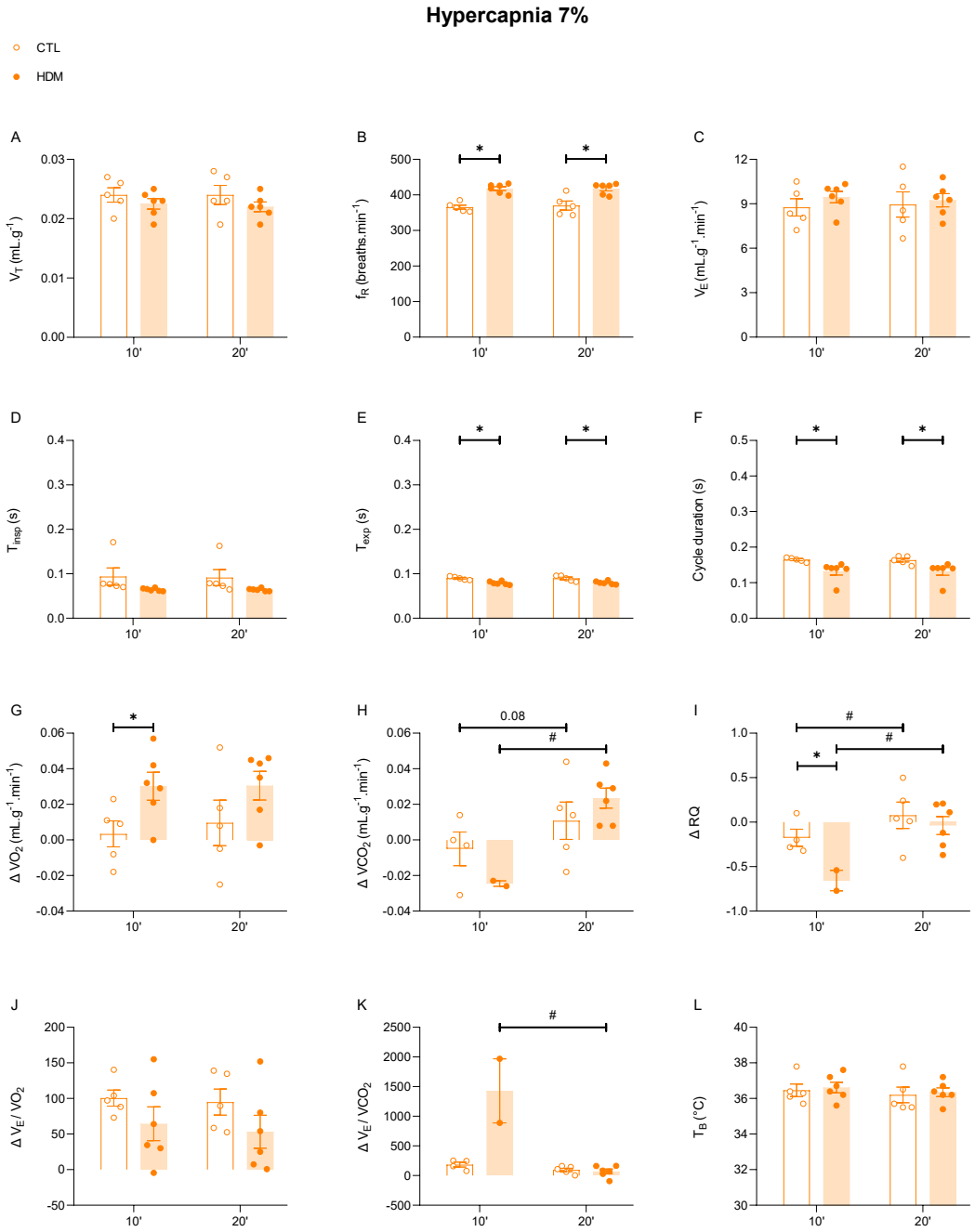
Hypercapnia 7%
CTL
HDM
A
B
C
D
E
F
G
H
I
J
K
L
V_T (mL.g^{-1})
f_R (breaths.min^{-1})
V_E (mL.g^{-1}.min^{-1})
T_{insp} (s)
T_{exp} (s)
Cycle duration (s)
Δ VO_2 (mL.g^{-1}.min^{-1})
Δ VCO_2 (mL.g^{-1}.min^{-1})
Δ RQ
Δ V_E/ VO_2
Δ V_E/ VCO_2
T_B (°C)
10'
20'
0.08

Figure 11.

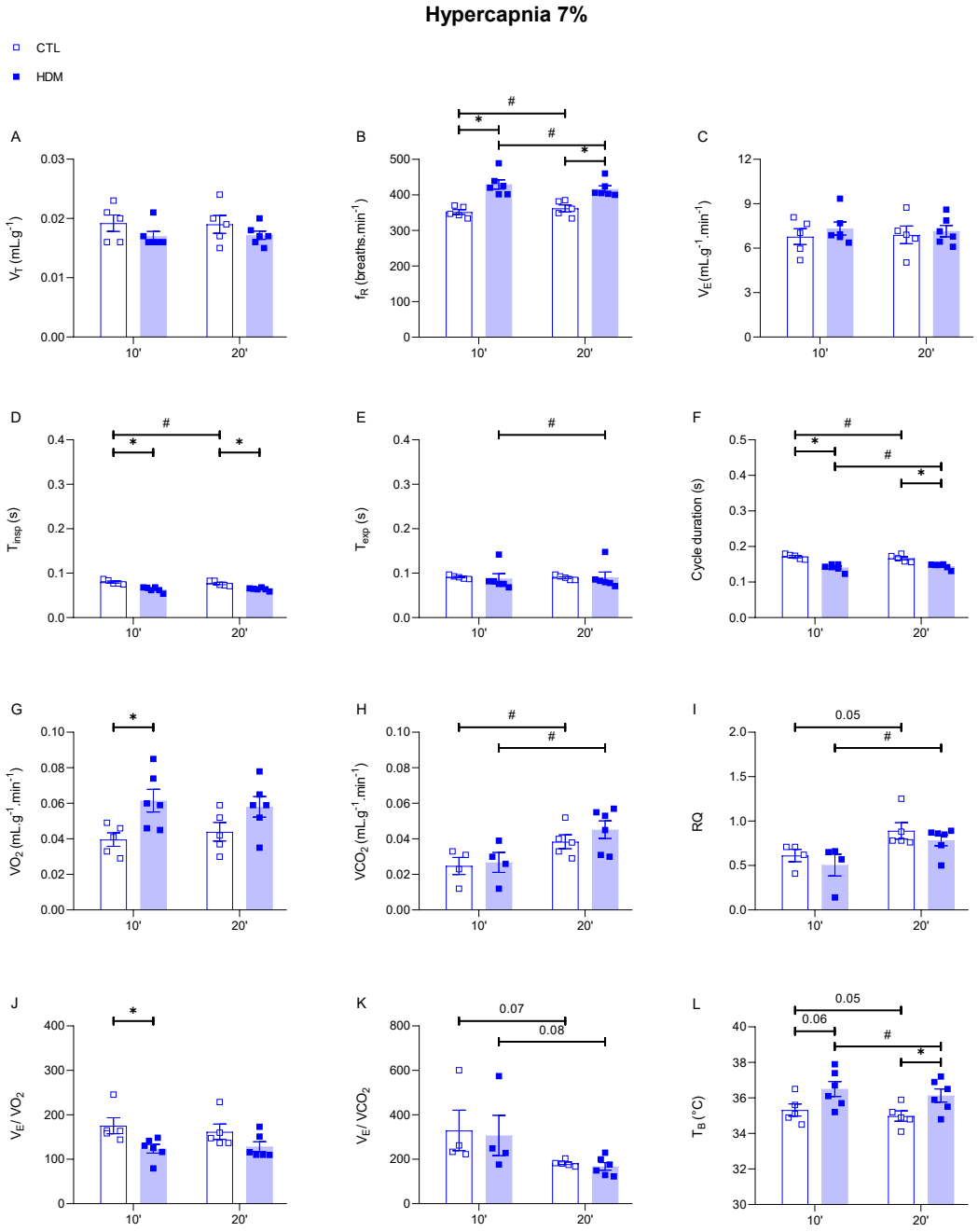
Hypercapnia 7%
CTL
HDM
A
B
C
D
E
F
G
H
I
J
K
L
V_T (mL.g^{-1})
f_R (breaths.min^{-1})
V_E(mL.g^{-1}.min^{-1})
T_{insp} (s)
T_{exp} (s)
Cycle duration (s)
VO_2 (mL.g^{-1}.min^{-1})
VCO_2 (mL.g^{-1}.min^{-1})
RQ
V_E/ VO_2
V_E/ VCO_2
T_B (°C)
10'
20'
0.05
0.07
0.08
0.06

Table 1. Two-Way ANOVA for female mice under room air.

	V_T	f_R	V_E
Treatment	F(1,9) = 0.6971 p = 0.4253	F(1,9) = 0.1937 p = 0,6701	F(1,9) = 0.1090 p = 0.7487
Time	F(1,9) = 0.9302 p = 0.36	F(1,9) = 1,2377 p = 0,2947	F(1,9) = 0.1954 p = 0.6688
Treatment vs time	F(1,9) = 0.1337 p = 0.7230	F(1,9) = 0.0072 p = 0.9341	F(1,9) = 0.0156 p = 0.9033
	T_{insp}	T_{exp}	**Cycle duration**
Treatment	F(1,9) = 3,3503 p = 0,1004	F(1,9) = 0,0812 p = 0,7821	F(1,9) = 0,1315 p = 0,7251
Time	F(1,9) = 0,0510 p = 0,8263	F(1,9) = 1,0828 p = 0,32521	F(1,9) = 1,1724 p = 0,307064
Treatment vs time	F(1,9) = 1,3856 p = 0,2693	F(1,9) = 0,4297 p = 0,528504	F(1,9) = 0,0851 p = 0,777039
	VO_2	VCO_2	**RQ**
Treatment	F(1,9) = 6.4451 p = 0.0317 *	F(1,9) = 4.2600 p = 0.0690	F(1,9) = 0.34848 p = 0.5694
Time	F(1,9) = 0.7605 p = 0.4058	F(1,9) = 3.4523 p = 0.0961	F(1,9) = 0.3694 p = 0.5583
Treatment vs time	F(1,9) = 0.2299 p = 0.6430	F(1,9) = 2.7227 p = 0.1333	F(1,9) = 3.3207 p = 0.1017
	V_E/VO_2	V_E/VCO_2	T_B
Treatment	F(1,9) = 3.7898 p = 0.0833	F(1,9) = 1.4724 p = 0.2560	F(1,9) = 0.1228 p = 0.7339
Time	F(1,9) = 0.3204 p = 0.585159	F(1,9) = 0.7595 p = 0.4082	F(1,9) = 14.11304 p = 0.0045 *
Treatment vs time	F(1,9) = 0.0552 p = 0.819428	F(1,9) = 0.4145 p = 0.5372	F(1,9) = 0.2181 p = 0.65153

Table 2. Post hoc time effect on VCO_2 in female mice under room air

Comparison	**Group**	**t**	**p**
Baseline vs recovery	Control	2.3750	0.0415 *
Baseline vs recovery	HDM	0.1542	0.8808

Table 3. Post hoc treatment effect on VCO_2 in female mice under room air

Comparison	Time	t	p
Control vs HDM	Baseline	2.7527	0.0223 *
Control vs HDM	Recovery	0.8306	0.4276

Table 4. Two-Way ANOVA for male mice under room air.

	V_T	f_R	V_E
Treatment	F(1,9) = 0.9591 p = 0.3529	F(1,9) = 2.4254 p = 0.1538	F(1,9) = 0.9941 p = 0.3447
Time	F(1,9) = 7.8562 p = 0.0206 *	F(1,9) = 2.3790 p = 0.1573	F(1,9) = 1.9510 p = 0.1959
Treatment vs time	F(1,9) = 3.7512 p = 0.0847	F(1,9) = 13.7085 p = 0.0049 *	F(1,9) = 0.3607 p = 0.5628
	T_{insp}	T_{exp}	Cycle duration
Treatment	F(1,9) = 13.1429 p = 0.0055	F(1,9) = 0.9474 p = 0.3557	F(1,9) = 2.5397 p = 2.5397
Time	F(1,9) = 0.00001 p = 0.9973	F(1,9) = 4.5246 p = 0.0623	F(1,9) = 2.9105 p = 0.1221
Treatment vs time	F(1,9) = 2.2198 p = 0.1704	F(1,9) = 16.5358 p = 0.0028 *	F(1,9) = 18.8281 p = 0.0018 *
	VO_2	VCO_2	RQ
Treatment	F(1,9) = 1.1892 p = 0.3038	F(1,9) = 0.0060 p = 0.9395	F(1,9) = 1.6826 p = 0.2268
Time	F(1,9) = 0.3152 p = 0.5881	F(1,9) = 2.1415 p = 0.1773	F(1,9) = 0.1779 p = 0.6830
Treatment vs time	F(1,9) = 2.1139 p = 0.1799	F(1,9) = 3.4743 p = 0.0952	F(1,9) = 0.0089 p = 0.9265
	V_E/VO_2	V_E/VCO_2	T_B
Treatment	F(1,9) = 1.6212 p = 0.2348	F(1,9) = 0.3127 p = 0.5896	F(1,9) = 0.0028 p = 0.9588
Time	F(1,9) = 0.3306 p = 0.5793	F(1,9) = 3.5908 p = 0.0906	F(1,9) = 12.2146 p = 0.0067 *
Treatment vs time	F(1,9) = 0.3198 p = 0.5855	F(1,9) = 2.1798 p = 0.1739	F(1,9) = 0.0037 p = 0.9527

Table 5. Post hoc treatment effect on T_{insp} in male mice under room air

Comparison	Time	t	p
Control vs HDM	Baseline	1.4573	0.1790
Control vs HDM	Recovery	4.4371	0.0016 *

Table 6. Post hoc time effect on VCO_2 in male mice under room air

Comparison	Group	t	p
Baseline vs recovery	Control	-0.2711	0.7923
Baseline vs recovery	HDM	2.4676	0.0357 *

Table 7. Post hoc time effect on V_E/VCO_2 in male mice under room air

Comparison	Group	t	p
Baseline vs recovery	Control	-0.2833	0.7833
Baseline vs recovery	HDM	-2.5002	0.0338 *

Table 8. Two-Way ANOVA for female mice under hypoxic conditions.

	V_T	f_R	V_E
Treatment	F(1,9) = 0.0048 p = 0.9462	F(1,9) = 2.2480 p = 0.1680	F(1,9) = 1.9048 p = 0,2008
Time	F(1,9) = 1.1015 p = 0.3212	F(1,9) = 2.4475 p = 0.1521	F(1,9) = 0.0612 p = 0,8101
Treatment vs time	F(1,9) = 0.0012 p = 0.9724	F(1,9) = 3.4947 p = 0.0943	F(1,9) = 1.4259 p = 0.2629
	T_{insp}	T_{exp}	**Cycle duration**
Treatment	F(1,9) = 0.1130 p = 0.7443	F(1,9) = 3.8565 p = 0.0811	F(1,9) = 0.7255 p = 0.4164
Time	F(1,9) = 0.1246 p = 0.0804	F(1,9) = 1.7671 p = 0.2164	F(1,9) = 0.7240 p = 0.4168
Treatment vs time	F(1,9) = 0.8814 p = 0.3723	F(1,9) = 0.0259 p = 0.8755	F(1,9) = 3.6065 p = 0.0900
	VO_2	VCO_2	**RQ**
Treatment	F(1,9) = 0.6183 p = 0.4518	F(1,9) = 0.0389 p = 0.8479	F(1,9) = 1.3442 p = 0.2761
Time	F(1,9) = 21.9765 p = 0.0011 *	F(1,9) = 9.6598 p = 0.0138 *	F(1,9) = 29.7573 p = 0.0004 *
Treatment vs time	F(1,9) = 2.8173 p = 0.1275	F(1,9) = 0.3367 p = 0.5770	F(1,9) = 1.6765 p = 0.2276
	V_E/VO_2	V_E/VCO_2	T_B
Treatment	F(1,9) = 2.7621 p = 0.1308	F(1,9) = 0.8951 p = 0.3688	F(1,9) = 0.4765 p = 0.5074
Time	F(1,9) = 11.1242 p = 0.0087 *	F(1,9) = 6.2606 p = 0.0364 *	F(1,9) = 58.1629 p = 0.00003 *
Treatment vs time	F(1,9) = 4.1599 p = 0.0718	F(1,9) = 0.1657 p = 0.6944	F(1,9) = 0.0109 p = 0.9189

Table 9. Post hoc time effect on f_R in female mice under hypoxic conditions.

Comparison	**Group**	**t**	**p**
10 min vs 20 min	Control	-0.2064	0.8410
10 min vs 20 min	HDM	2.5466	0.0313 *

Table 10. Post hoc treatment effect on T_{insp} in female mice under hypoxic conditions.

Comparison	Time	t	p
Control vs HDM	10 min	2.4573	0.0363 *
Control vs HDM	20 min	-0.1925	0.8515

Table 11. Two-Way ANOVA for male mice under hypoxic conditions.

	V_T	f_R	V_E
Treatment	F(1,9) = 0.8877 p = 0.3706	F(1,9) = 8.2104 p = 0.0186 *	F(1,9) = 17.3502 p = 0.0024 *
Time	F(1,9) = 6.8554 p = 0.0278 *	F(1,9) = 16.0201 p = 0.0030 *	F(1,9) = 0.2091 p = 0.6582
Treatment vs time	F(1,9) = 0.2366 p = 0.6382	F(1,9) = 0.9412 p = 0.3572	F(1,9) = 0.5035 p = 0.4959
	T_{insp}	**T_{exp}**	**Cycle duration**
Treatment	F(1,9) = 6.3012 p = 0.0332 *	F(1,9) = 5.5557 p = 0.0428 *	F(1,9) = 8.4728 p = 0.0172 *
Time	F(1,9) = 16.4610 p = 0.0028 *	F(1,9) = 0.0949 p = 0.7649	F(1,9) = 20.5957 p = 0.0014 *
Treatment vs time	F(1,9) = 3.0525 p = 0.1145	F(1,9) = 0.0435 p = 0.8393	F(1,9) = 6.1503 p = 0.0349 *
	VO_2	**VCO_2**	**RQ**
Treatment	F(1,9) = 0.7895 p = 0.3973	F(1,9) = 0.0188 p = 0.8938	F(1,9) = 0.7565 p = 0.4069
Time	F(1,9) = 8.8500 p = 0.0155 *	F(1,9) = 69.3211 p = 0.00001 *	F(1,9) = 12.4812 p = 0.0063 *
Treatment vs time	F(1,9) = 0.0275 p = 0.8718	F(1,9) = 0.3296 p = 0.5799	F(1,9) = 0.6173 p = 0.4522
	V_E/VO_2	**V_E/VCO_2**	**T_B**
Treatment	F(1,9) = 4.0278 p = 0.0756	F(1,9) = 2.9861 p = 0.1180	F(1,9) = 0.8094 p = 0.3917
Time	F(1,9) = 3.3877 p = 0.0988	F(1,9) = 11.5787 p = 0.0078 *	F(1,9) = 13.4873 p = 0.0051 *
Treatment vs time	F(1,9) = 0.3099 p = 0.5912	F(1,9) = 1.5988 p = 0.2378	F(1,9) = 2.7045 p = 0.1344

Table 12. Two-Way ANOVA for female mice under hypercapnic conditions.

	V_T	f_R	V_E
Treatment	F(1,9) = 1.2643 p = 0.2899	F(1,9) = 23.9543 p = 0.0008 *	F(1,9) = 0.4073 p = 0.5392
Time	F(1,9) = 0.1124 p = 0.7450	F(1,9) = 0.2366 p = 0.6382	F(1,9) = 0.0015 p = 0.9695
Treatment vs time	F(1,9) = 0.2419 p = 0.6345	F(1,9) = 0.3185 p = 0.5862	F(1,9) = 0.6777 p = 0.4316
	T_{insp}	T_{exp}	**Cycle duration**
Treatment	F(1,9) = 2.7471 p = 0.1318	F(1,9) = 18.5698 p = 0.0019 *	F(1,9) = 6.1796 p = 0.0346 *
Time	F(1,9) = 1.6663 p = 0.2289	F(1,9) = 0.0074 p = 0.9332	F(1,9) = 0.2235 p = 0.6476
Treatment vs time	F(1,9) = 1.4908 p = 0.2531	F(1,9) = 0.0582 p = 0.8146	F(1,9) = 0.0531 p = 0.8228
	VO_2	VCO_2	**RQ**
Treatment	F(1,9) = 0.6769 p = 0.4318	F(1,9) = 2.8464 p = 0.1239	F(1,9) = 2.6364 p = 0.1404
Time	F(1,9) = 0.4397 p = 0.5238	F(1,9) = 21.4662 p = 0.0057 *	F(1,9) = 159.2306 p = 0.00007 *
Treatment vs time	F(1,9) = 0.3766 p = 0.5545	F(1,9) = 4.4377 p = 0.0893	F(1,9) = 3.3197 p = 0.1312
	V_E/VO_2	V_E/VCO_2	T_B
Treatment	F(1,9) = 0.2202 p = 0.6500	F(1,9) = 2.7936 p = 0.1345	F(1,9) = 0.1172 p = 0.7398
Time	F(1,9) = 0.4770 p = 0.5072	F(1,9) = 20.7057 p = 0.0049 *	F(1,9) = 5.3463 p = 0.0460 *
Treatment vs time	F(1,9) = 0.0530 p = 0.8230	F(1,9) = 1.0172 p = 0.3559	F(1,9) = 0.00002 p = 0.9962

Table 13. Two-Way ANOVA for male mice under hypercapnic conditions.

	V_T	f_R	V_E
Treatment	F(1,9) = 1.6562 p = 0.2302	F(1,9) = 20.7340 p = 0.0013 *	F(1,9) = 0.3551 p = 0.5658
Time	F(1,9) = 0.0364 p = 0.8527	F(1,9) = 0.2485 p = 0.6300	F(1,9) = 0.0361 p = 0.8534
Treatment vs time	F(1,9) = 0.2451 p = 0.6323	F(1,9) = 16.1658 p = 0.0030 *	F(1,9) = 1.1035 p = 0.3208
	T_{insp}	T_{exp}	**Cycle duration**
Treatment	F(1,9) = 24.6126 p = 0.0007 *	F(1,9) = 0.0086 p = 0.9281	F(1,9) = 24.6266 p = 0.0007 *
Time	F(1,9) = 2.9213 p = 0.1215	F(1,9) = 1.6851 p = 0.2265	F(1,9) = 0.1401 p = 0.7167
Treatment vs time	F(1,9) = 9.3375 p = 0.0136 *	F(1,9) = 7.8819 p = 0.0204 *	F(1,9) = 19.4735 p = 0.0016 *
	VO_2	VCO_2	**RQ**
Treatment	F(1,9) = 6.2305 p = 0.0340 *	F(1,9) = 0.92098 p = 0.3626	F(1,9) = 1.2474 p = 0.2958
Time	F(1,9) = 0.0139 p = 0.9084	F(1,9) = 22.0916 p = 0.0025 *	F(1,9) = 11.0487 p = 0.0111 *
Treatment vs time	F(1,9) = 1.3438 p = 0.2761	F(1,9) = 0.0987 p = 0.7629	F(1,9) = 0.000001 p = 0.9989
	V_E/VO_2	V_E/VCO_2	T_B
Treatment	F(1,9) = 5.5015 p = 0.0436 *	F(1,9) = 0.1054 p = 0.7534	F(1,9) = 5.1737 p = 0.0489 *
Time	F(1,9) = 0.3462 p = 0.5706	F(1,9) = 8.1151 p = 0.0230 *	F(1,9) = 10.9138 p = 0.0091 *
Treatment vs time	F(1,9) = 1.4821 p = 0.2543	F(1,9) = 0.0101 p = 0.9223	F(1,9) = 0.0155 p = 0.9034